Arch Appl Mech (2017) 87:15–40
DOI 10.1007/s00419-016-1172-2

ORIGINAL

Faisal M. Mukhtar

Free vibration analysis of orthotropic plates by differential transform and Taylor collocation methods based on a refined plate theory

Received: 5 February 2016 / Accepted: 7 August 2016 / Published online: 26 August 2016

Abstract Based on the two-variable refined plate theory, free vibration of orthotropic plates is analyzed using the differential transform method (DTM) and the Taylor collocation method (TCM). The refined plate theory outperforms the classical plate theory, and its formulation is simpler than those of other higher-order theories. Without the need for any shear correction factor, the theory performs reliably. The plates considered have two opposite edges simply supported (Levy plates). The first part of the analysis considers three combinations of clamped, simply supported and free edge conditions for the other two edges, keeping one of them simply supported. Detailed formulations of DTM and TCM for the free vibration analysis are given and, consequently, used to predict the frequency parameters and the effect of various factors ranging from geometric to material parameters. Next, the paper presents analysis of some cases, the multi-span plates and plates with stepped thickness and end rotational springs, whose analytical solutions are not readily available, particularly based on the two-variable refined plate theory. In order to verify the results, formulations of three more plate theories, namely the classical or Kirchhoff plate theory, the first-order shear deformation theory of Mindlin and the high-order shear deformation theory of Sayyad and Gugal, were implemented and solved using the proposed methods.

Keywords Differential transform method · Taylor collocation method · Free vibration analysis · Orthotropic plates · Refined plate theory

1 Introduction

Plates are important structural components that have many applications in civil, aerospace, automobile and marine structures, etc. Depending on the purpose, these plates may be isotropic or orthotropic, with the latter becoming increasingly adopted due to its numerous advantages. Both static and dynamic analyses of these elements require that certain theory or, more precisely, plate theory be used to arrive at the governing equations subject to some boundary conditions. Starting from the classical plate theory (CPT), several works have been reported and quite a number of other higher-order theories and their variations exist today.

The CPT or the Kirchhoff plate theory [1] is very appealing in terms of simplicity and ease of solution. It has been successfully applied to free vibration analysis of orthotropic plates in [2–7]. However, the fact that it does not take into account the effect of transverse shear stresses limits its application to thin plates. It is also worth mentioning that the effect of shear stresses is more pronounced in orthotropic plates. As a result, natural frequencies are overestimated by the CPT in case of thick/orthotropic plates. If a more reliable solution is needed, other plate theories that incorporate shear deformation effects need to be sought. A number of such shear deformation theories are available in the literature, including the first-order shear deformation theory

Faisal M. Mukhtar
Department of Civil and Environmental Engineering, King Fahd University of Petroleum & Minerals, 31261 Dhahran, Saudi Arabia
E-mail: faisalmu@kfupm.edu.sa

(FSDT) [8–10] and the higher-order shear deformation theories (HSDT) [11–20]. Typical instances where free vibration analyses of orthotropic plates were carried out based on these theories can be found in [21–24] based on the FSDT and in [25–28] based on the HSDT. The FSDT assumes a constant distribution of shear stress across the plate's thickness, thereby violating zero-stress condition on the plate's top and bottom surfaces. In order to take care of this inconsistency, use of a correction factor becomes necessary in the FSDT. On the other hand, the HSDT do not require the use of such correction factor and they, still, satisfy the zero-traction boundary condition at the top and bottom surfaces of the plate. But, this happens at the expense of more complex formulation, involving several unknowns, that becomes inconvenient to handle. Such set-backs encountered in form of lesser accuracy in the CPT and the inconveniencies in formulating the higher-order theories can be well taken care of by the adoption of the two-variable refined plate theory (RPT) of Shimpi [29], which was later extended by Shimpi and Patel [30] to orthotropic plates. The RPT is very similar to the CPT, and it still accounts for shear stress distribution that satisfies zero-traction boundaries without the need for any correction factor. RPT expresses the governing equations in terms of only two unknown functions. Zig-zag and layer-wise theories of plates [31] are other useful plate theories whose recent applications to laminate glass and solar panels prove successful. Detailed analysis of free vibrations of functionally graded plates has been performed using several variants of plate models in [32].

Each of the aforementioned theories yields a set of governing differential equations, some of which require advanced methods of solution. Consequently, several studies reported the application of various methods to analyze free vibration of orthotropic plates. Some of these include the works reported in [33,34] based on the Navier's method, [35] based on the Levy's method, [36–38] based on the finite element method, [36,39–41] based on the Rayleigh–Ritz method, [42–44] based on the state–space method, [36,45] based on the differential quadrature method, [46–48] based on the meshless method including the RBF, [49,50] based on the Galerkin method, [51,52] based on the discrete singular convolution (DSC) method, [53] based on the extended Kantorovich method, [54] based on the mixed variational formulations and [7,55,56] based on the exact solutions. A more comprehensive review of recent literature on free vibration analysis of general composite plates can be found in the work of Sayyad and Ghugal [57].

As evident in the above and other numerous studies on the use of various solution tools and theories for free vibration of orthotropic plates, it can be noticed that the application of differential transform method (DTM) and Taylor collocation method (TCM) for free vibration of orthotropic plates is not popular, if any. Works such as those reported in [58,59] utilized the DTM only for isotropic and not for orthotropic plates. As for the TCM, most of the published research on its application addresses other problems but not free vibration of orthotropic plates.

This paper has dual objectives, one of which is to present a study based on a very efficient and relatively simple theory, the two-variable refined plate theory (RPT) [30], which outperforms the CPT. In addition, the inconveniencies in formulating the first-order and higher-order shear deformation theories can be avoided by the use of the refined plate theory. The theory allows quadratic shear stress distribution that satisfies zero-traction boundaries without the need for any correction factor. Additionally, as the name implies, the two-variable RPT expresses the governing equations in terms of only two unknown functions, contrary to the need for several functions in many of the higher-order theories. The similarity, in some ways, of the refined theory with the CPT speaks enough about its simplicity. The second objective of the paper is to present two solution schemes, the DTM and TCM, having some similarities with respect to their origin and to illustrate how they can, conveniently, be used in the analysis of free vibrations of the orthotropic plates based on the RPT. The work reported in [30] presents some results for free vibration of simply supported square orthotropic plate based on this theory. Later, Thai and Kim [35] extended the analysis to consider other boundary conditions. However, aside from the simply supported square plate, results of the work reported in [35] has been presented without further verification with other methods. Hence, the present work will have a secondary benefit of serving as a verification of some of the results reported in [35]. But, in addition, some cases whose analytical solutions are not readily available, particularly based on the two-variable refined plate theory, are also analyzed. In order to verify the results for those cases with no analytical solution, formulation of three more plate theories, the CPT, the FSDT [10,60,61] and the HSDT [62], was implemented and solved using both the DTM and TCM. The robustness and competitiveness of DTM and TCM in providing reliable results make them good alternatives to the analytical solutions.

2 Two-variable refined plate theory (RPT) for orthotropic plate [30]

The two-variable RPT of Shimpi and Patel [30] has many attractive features that make it competitive with other well-established and robust plate theories. First, the theory is similar to the CPT and, hence, it is simple.

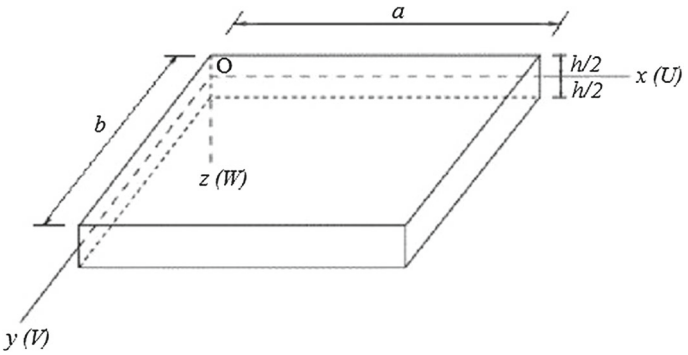

Fig. 1 Geometry and orientation of the plate considered

In addition, there is no need for shear correction factor as required in some shear deformation theories, and it still takes into account the effect of shear stress distribution that satisfies zero-traction boundaries. This way, the RPT takes care of both the lesser accuracy in the CPT and the complexities in formulating the first-order and higher-order shear deformation theories. Detailed derivation of RPT for orthotropic plates can be found in [30], but its overview is given as follows.

2.1 Coordinate system and orthotropic plate configuration

The plate under consideration has dimensions of $a \times b \times h$ and is oriented with respect to a right-handed Cartesian coordinate system as shown in Fig. 1. The displacement components U, V and W corresponding to the x, y and z coordinate directions, respectively, are shown in bracket. For free vibration, the top and bottom surfaces are free. On the other hand, convenient boundary conditions can be applied at the edges $x = 0$, $x = a$, $y = 0$ and $y = b$.

2.2 Displacements, constitutive equations and stress resultants

According to CPT, the displacement components are given by Eq. (1).

$$U = -z\frac{\partial W}{\partial x};\ V = -z\frac{\partial W}{\partial y};\ W = W_b \tag{1}$$

where W_b is the transverse displacement due to bending effect alone.

It is clear from Eq. (1) that, by default, any subsequent formulation in terms of U, V and W based on CPT neglects the effect of transverse shear. On the contrary, the RPT assumes that both U, V and W consists of bending components (U_b, V_b and W_b, respectively) and shear components (U_s, V_s and W_s, respectively) thus.

$$U = U_b + U_s;\ V = V_b + V_s;\ W = W_b + W_s \tag{2}$$

where

$$U_b = -z\frac{\partial W_b}{\partial x};\ U_s = h\left(\frac{1}{4}\left(\frac{z}{h}\right) - \frac{5}{3}\left(\frac{z}{h}\right)^3\right)\frac{\partial W_s}{\partial x};\ V_b = -z\frac{\partial W_b}{\partial y};\ V_s = h\left(\frac{1}{4}\left(\frac{z}{h}\right) - \frac{5}{3}\left(\frac{z}{h}\right)^3\right)\frac{\partial W_s}{\partial y}$$

The six independent strain components are obtained by using the displacement expressions given by Eq. (2) in the following strain-displacement relations.

$$\varepsilon_x = \frac{\partial U}{\partial x};\ \varepsilon_y = \frac{\partial V}{\partial y};\ \varepsilon_z = \frac{\partial W}{\partial z};\ \gamma_{xy} = \frac{\partial V}{\partial x} + \frac{\partial U}{\partial y};\ \gamma_{yz} = \frac{\partial W}{\partial y} + \frac{\partial V}{\partial z};\ \gamma_{zx} = \frac{\partial U}{\partial z} + \frac{\partial W}{\partial x} \tag{3}$$

Equation (3) can be substituted in the constitutive equations to obtain the corresponding stresses given by Eq. (4).

$$\boldsymbol{\sigma} = \overline{\boldsymbol{Q}}\,\boldsymbol{\varepsilon} \tag{4}$$

where $\sigma = \left[\sigma_x, \sigma_y, \tau_{xy}, \tau_{yz}, \tau_{zx}\right]^T$; $\varepsilon = \left[\varepsilon_x, \varepsilon_y, \gamma_{xy}, \gamma_{yz}, \gamma_{zx}\right]^T$ and $\overline{\boldsymbol{Q}}$ is a 5×5 matrix whose elements are

$$\overline{Q}_{11} = Q_{11} = \frac{E_1}{1 - \nu_{12}\nu_{21}}; \quad \overline{Q}_{12} = \overline{Q}_{21} = Q_{12} = \frac{\nu_{12}E_1}{1 - \nu_{12}\nu_{21}}; \quad \overline{Q}_{22} = Q_{22} = \frac{E_2}{1 - \nu_{12}\nu_{21}}$$

$\overline{Q}_{33} = Q_{66} = G_{12}$; $\overline{Q}_{44} = Q_{44} = G_{23}$; $\overline{Q}_{55} = Q_{55} = G_{31}$ and $\overline{Q}_{ij} = 0$ for other combinations of i and j.

$E_i\ (i = 1, 2)$, $G_{ij}\ (i, j = 1, 2, 3\ \&\ i \neq j)$ and $\nu_{ij}(i, j = 1, 2\ \&\ i \neq j)$ are the Young's modulus, shear modulus and Poisson's ratio, respectively. The subscripts 1, 2 and 3 correspond to the three coordinate directions, x, y and z, respectively.

Expressions for the stress resultants (moments and shear forces) can be obtained from Eq. (5a) to arrive at Eq. (5b).

$$\begin{Bmatrix} M_x^b \\ M_y^b \\ M_{xy}^b \\ M_x^s \\ M_y^s \\ M_{xy}^s \\ Q_x \\ Q_y \end{Bmatrix} = \int_{z=-h/2}^{z=h/2} \begin{Bmatrix} \sigma_x z \\ \sigma_y z \\ \tau_{xy} z \\ \sigma_x \left(-\frac{1}{4}z + \frac{5}{3}z\left(\frac{z}{h}\right)^2\right) \\ \sigma_y \left(-\frac{1}{4}z + \frac{5}{3}z\left(\frac{z}{h}\right)^2\right) \\ \tau_{xy} \left(-\frac{1}{4}z + \frac{5}{3}z\left(\frac{z}{h}\right)^2\right) \\ \tau_{zx} \\ \tau_{yz} \end{Bmatrix} \mathrm{d}z \tag{5a}$$

$$\begin{Bmatrix} M_x^b \\ M_y^b \\ M_{xy}^b \\ M_x^s \\ M_y^s \\ M_{xy}^s \\ Q_x \\ Q_y \end{Bmatrix} = \begin{bmatrix} -D_{11} & -D_{12} & 0 & 0 & 0 & 0 & 0 & 0 \\ -D_{12} & -D_{22} & 0 & 0 & 0 & 0 & 0 & 0 \\ 0 & 0 & -D_{66} & 0 & 0 & 0 & 0 & 0 \\ 0 & 0 & 0 & -\frac{1}{84}D_{11} & -\frac{1}{84}D_{12} & 0 & 0 & 0 \\ 0 & 0 & 0 & -\frac{1}{84}D_{12} & -\frac{1}{84}D_{22} & 0 & 0 & 0 \\ 0 & 0 & 0 & 0 & 0 & -\frac{1}{84}D_{66} & 0 & 0 \\ 0 & 0 & 0 & 0 & 0 & 0 & A_{55} & 0 \\ 0 & 0 & 0 & 0 & 0 & 0 & 0 & A_{44} \end{bmatrix} \begin{Bmatrix} \frac{\partial^2 W_b}{\partial x^2} \\ \frac{\partial^2 W_b}{\partial y^2} \\ 2\frac{\partial^2 W_b}{\partial x \partial y} \\ \frac{\partial^2 W_s}{\partial x^2} \\ \frac{\partial^2 W_s}{\partial y^2} \\ 2\frac{\partial^2 W_s}{\partial x \partial y} \\ \frac{\partial W_s}{\partial x} \\ \frac{\partial W_s}{\partial y} \end{Bmatrix} \tag{5b}$$

The material parameters are

$$D_{11} = \frac{Q_{11}h^3}{12}; D_{22} = \frac{Q_{22}h^3}{12}; D_{12} = \frac{Q_{12}h^3}{12}; D_{66} = \frac{Q_{66}h^3}{12}; A_{44} = \frac{5Q_{44}h}{6}; A_{55} = \frac{5Q_{55}h}{6}$$

2.3 Governing equations of motion

In deriving the equations of motion based on RPT, expressions for the kinetic and potential energies are, firstly, written as in Eqs. (6) and (7), respectively [30,35].

$$E_k = \frac{1}{2}\int_{-\frac{h}{2}}^{\frac{h}{2}}\int_0^b\int_0^a \rho\left[\left(\frac{\partial U_b}{\partial t} + \frac{\partial U_s}{\partial t}\right)^2 + \left(\frac{\partial V_b}{\partial t} + \frac{\partial V_s}{\partial t}\right)^2 + \left(\frac{\partial W_b}{\partial t} + \frac{\partial W_s}{\partial t}\right)^2\right]\mathrm{d}x\,\mathrm{d}y\,\mathrm{d}z \tag{6}$$

$$U = \frac{1}{2}\int_{-\frac{h}{2}}^{\frac{h}{2}}\int_0^b\int_0^a \rho\left[\sigma_x\varepsilon_x + \sigma_y\varepsilon_y + \tau_{xy}\gamma_{xy} + \tau_{yz}\gamma_{yz} + \tau_{zx}\gamma_{zx}\right]\mathrm{d}x\,\mathrm{d}y\,\mathrm{d}z \tag{7}$$

Equations (6) and (7) are substituted in Eq. (8), written using Hamilton's principle. Integrating the resulting equation by parts, and due to the independence of δW_b and δW_s, their coefficients can be collected separately which give the governing equations of motion, given by Eq. (9), for free vibration of orthotropic plates.

$$\int_0^t \delta\left(E_k - U\right)\mathrm{d}t = 0 \tag{8}$$

$$L_1[W_b] + I_0\left(\frac{\partial^2 W_b}{\partial t^2} + \frac{\partial^2 W_s}{\partial t^2}\right) = q \tag{9a}$$

$$L_1[W_s] + 84\left(L_2[W_s] + I_0\left(\frac{\partial^2 W_b}{\partial t^2} + \frac{\partial^2 W_s}{\partial t^2}\right)\right) = 84q \tag{9b}$$

where the linear differential operators L_1 and L_2 are defined thus

$$L_1[\cdots] = D_{11}\frac{\partial^4(\cdots)}{\partial x^4} + 2(D_{12} + 2D_{66})\frac{\partial^4(\cdots)}{\partial x^2 \partial y^2} + D_{22}\frac{\partial^4(\cdots)}{\partial y^4} - I_2\frac{\partial^2}{\partial t^2}(\nabla^2(\cdots))$$

$$L_2[\cdots] = -\left(A_{55}\frac{\partial^2(\cdots)}{\partial x^2} + A_{44}\frac{\partial^2(\cdots)}{\partial y^2}\right)$$

I_0 and I_2 are inertias given by ρh and $\rho h^3/12$, respectively.

For free vibration, the external transverse load $q = 0$.

It is important, at this point, to discuss the concept of consistency which arises when deciding the conformity of the various plate theories/models with linear three-dimensional theory of elasticity. This is of concern because there are several plate theories, including the RPT presented in this work, that are based on some priori assumptions which may result in system of equations that violate the elasticity theory. Interestingly, however, Shimpi [29] has already reported that the RPT is variationally consistent. Details of the consistent approach are well addressed by Kienzler [63], where he derived some consistent plate theories from the basic equations of three-dimensional linear theory of elasticity by applying the uniform-approximation technique which, depending on the order of the approximation chosen, yields a set of governing partial differential equations without invoking any *priori* assumptions or shear correction factors. Some recent works where similar idea was used include [64] where the concept is applied to anisotropic materials and [65] where comparison of various linear plate theories in light of consistent second-order approximation is made.

2.4 Free vibration equations for the orthotropic plate under consideration

The present study considers rectangular orthotropic plates with the two opposite boundaries, parallel to the x-axis (i.e., $y = 0$ and $y = b$), simply supported (i.e., Levy plates). The first part of the analysis considers a case of three combinations of clamped (C), simply supported (S) and free (F) edge conditions on the two remaining boundaries (i.e., at $x = 0$ and $x = a$), keeping one of them to be simply supported. Consequently, plates with one end simply supported and the other free, one end simply supported and the other clamped, and both ends simply supported are referenced as SF, SC and SS plates, respectively. Next, multi-span plates and plates with stepped thickness and end rotational springs, whose analytical solutions are not readily available, particularly based on the two-variable refined plate theory are also analyzed in this work.

Assuming a solution, given by Eq. (10), for the transverse displacement components W_b and W_s, it can easily be seen that the boundary conditions of zero displacement and zero moment at $y = 0$ and $y = b$ are automatically satisfied [35].

$$W_b(x, y, t) = \sum_{n=1}^{\infty} w_b(x)\, e^{i\omega_n t} \sin(\beta y) \tag{10a}$$

$$W_s(x, y, t) = \sum_{n=1}^{\infty} w_s(x)\, e^{i\omega_n t} \sin(\beta y) \tag{10b}$$

where the unknown functions $w_b(x)$ and $w_s(x)$ need to be determined. $\beta = n\pi/b$ and the natural frequency of the nth mode is denoted by ω_n.

Substituting Eq. (10) in the two governing equations given by Eq. (9) yields the system of two coupled equations given by Eq. (11). Similarly, the boundary conditions can be written as given in Table 1.

$$D_{11}w_b'''' - \left[2\beta^2(D_{12} + 2D_{66}) - \omega_n^2 I_2\right]w_b'' - \left[\omega_n^2 I_0 + \omega_n^2 I_2\beta^2 - D_{22}\beta^4\right]w_b - \omega_n^2 I_0 w_s = 0 \tag{11a}$$

$$D_{11}w_s'''' - \left[84A_{55} + 2\beta^2(D_{12} + 2D_{66}) - \omega_n^2 I_2\right]w_s'' - \left[84\omega_n^2 I_0 + \beta^2\left(\omega_n^2 I_2 - D_{22}\beta^2 - 84A_{44}\right)\right]w_s - 84\omega_n^2 I_0 w_b = 0 \tag{11b}$$

where $(\cdots)' = \frac{\mathrm{d}(\cdots)}{\mathrm{d}x}$, $(\cdots)'' = \frac{\mathrm{d}^2(\cdots)}{\mathrm{d}x^2}$ and so on.

Table 1 Boundary conditions for the SS, SC and SF plates

Boundary condition	Boundary type		
	C	S	F
w_b	0	0	–
w_s	0	0	–
w_b'	0	–	–
w_s'	0	–	–
$-D_{11}w_b'' + D_{12}\beta^2 w_b$	–	0	0
$-(1/84)\left(D_{11}w_s'' - D_{12}\beta^2 w_s\right)$	–	0	0
$-D_{11}w_b''' + \left(\left(D_{12}+4D_{66}\right)\beta^2 - I_2\omega_n^2\right)w_b'$	–	–	0
$-D_{11}w_s''' + \left(\left(D_{12}+4D_{66}\right)\beta^2 - I_2\omega_n^2 + 84A_{55}\right)w_s'$	–	–	0

In the subsequent analyses, use is made of a non-dimensional space variable $\bar{x} = x/a$, where a is the x-directional dimension of the plate shown in Fig. 1. Hence, $0 \leq \bar{x} \leq 1$.

3 Differential transform method (DTM)

Originally proposed by Zhou [66], the DTM is a semi-analytical method that, in recent decades, gained recognition for solving problems governed by differential equations. Its concept stems from the Taylor series expansion, and solution of the original problem is approximated in form of polynomials. However, unlike in the Taylor series method, symbolic evaluation of the derivatives is avoided in DTM. Instead, they are obtained by some recursive relations obtainable from the transformed governing equations.

3.1 Fundamentals of DTM

Consider an analytic function $w(x)$ that is sufficiently differentiable within the domain of interest. By definition, the differential transformation of $w(x)$ near the point $x = x_0$ is $W(k)$ given by Eq. (12). Conversely, the differential inverse transform of $W(k)$ is given by Eq. (13). Due to the consequence of Eq. (12), Eq. (13) can be rewritten in the form given by Eq. (14); the Taylor series expansion.

$$W(k) = \frac{1}{k!}\left(\frac{\mathrm{d}^k w(x)}{\mathrm{d}x^k}\right)_{x=x_0} \tag{12}$$

$$w(x) = \sum_{k=0}^{\infty}(x - x_0)^k W(k) \tag{13}$$

$$w(x) = \sum_{k=0}^{\infty}\frac{(x - x_0)^k}{k!}\left(\frac{\mathrm{d}^k w(x)}{\mathrm{d}x^k}\right)_{x=x_0} \tag{14}$$

For an integer $\bar{N}$ large enough to result in a negligibly small value of the summation $\sum_{k=\bar{N}+1}^{\infty}(x - x_0)^k W(k)$, the approximation of the original function (in our case, the solution) given by Eq. (13) can be truncated and rewritten as shown in Eq. (15). This way, $\bar{N}$ represents the number of terms sufficient enough for the series convergence.

$$w(x) = \sum_{k=0}^{\bar{N}}(x - x_0)^k W(k) \tag{15}$$

Since the aim of DTM is to transform the original differential equation(s) into recursive formulas needed to evaluate the terms $W(k)\left\{k, 0, \bar{N}\right\}$, some basic mathematical operations required in the transformation are given by Eqs. (16) to (23).

$$
\begin{aligned}
& w(x) && \xrightarrow{\text{transformsto}} && W(k) && (16)\\
& cw(x) && && cW(k) && (17)\\
& \alpha_1 w_1(x) + \alpha_2 w_2(x) + \cdots + \alpha_n w_n(x) && && \alpha_1 W_1(k) + \alpha_2 W_2(k) + \cdots + \alpha_n W_n(k) && (18)\\
& \frac{\mathrm{d}w(x)}{dx} && && (k+1)\, W(k+1) && (19)\\
& \frac{\mathrm{d}^2 w(x)}{\mathrm{d}x^2} && && (k+1)(k+2)\, W(k+2) && (20)\\
& \frac{\mathrm{d}^3 w(x)}{\mathrm{d}x^3} && && (k+1)(k+2)(k+3)\, W(k+3) && (21)\\
& \frac{\mathrm{d}^4 w(x)}{\mathrm{d}x^4} && && (k+1)(k+2)(k+3)(k+4)\, W(k+4) && (22)\\
& \vdots && && \vdots\\
& \vdots && && \vdots\\
& \frac{\mathrm{d}^n w(x)}{\mathrm{d}x^n} && && \frac{(k+n)!}{k!} W(k+n) && (23)
\end{aligned}
$$

3.2 Free vibration analysis based on DTM

This section presents the application of DTM for the free vibration analysis of orthotropic plates based on the two governing equations given by Eq. (11). For that purpose, the bending and shear displacement components of the transverse displacement are approximated around $\bar{x} = \bar{x}_0$ as follows.

$$
w_b(\bar{x}) = \sum_{k=0}^{\bar{N}} (\bar{x} - \bar{x}_0)^k W_b(k)\,; \quad w_s(\bar{x}) = \sum_{k=0}^{\bar{N}} (\bar{x} - \bar{x}_0)^k W_s(k) \tag{24}
$$

It should be noted that $W_b(k)$ and $W_s(k)$ in the present section are constants and are, therefore, different from $W_b(x)$ and $W_s(x)$ appearing in the previous sections (which are continuous functions of the space variable x).

Substituting the transform values of Eqs. (16) to (23) in Eq. (11) results in the following equations.

$$
W_b(k+4) = \frac{c_1 (k+1)(k+2) W_b(k+2) + c_2 W_b(k) + c_3 W_s(k)}{(k+1)(k+2)(k+3)(k+4)} \tag{25a}
$$

$$
W_s(k+4) = \frac{c_4 (k+1)(k+2) W_s(k+2) + c_5 W_s(k) + c_6 W_b(k)}{(k+1)(k+2)(k+3)(k+4)} \tag{25b}
$$

where

$$
c_1 = \frac{\left(2\beta^2 (D_{12} + 2D_{66}) - \omega_n^2 I_2\right)}{D_{11}}, c_2 = \frac{\left(\omega_n^2 I_0 + \omega_n^2 I_2 \beta^2 - D_{22}\beta^4\right)}{D_{11}}, \tag{26a}
$$

$$
c_3 = \frac{\omega_n^2 I_0}{D_{11}}, c_4 = \frac{\left(84A_{55} + 2\beta^2 (D_{12} + 2D_{66}) - \omega_n^2 I_2\right)}{D_{11}}, \tag{26b}
$$

$$
c_5 = \frac{\left(84\omega_n^2 I_0 + \beta^2 \left(\omega_n^2 I_2 - D_{22}\beta^2 - 84A_{44}\right)\right)}{D_{11}}, \quad c_6 = \frac{84\omega_n^2 I_0}{D_{11}} \tag{26c}
$$

Since the three cases considered in the first part of the work are the SF, SS and SC plates, the boundary conditions at $\bar{x} = 0$ (i.e., the S-type boundary) are, therefore, common to all the three plate cases. Consequently, the displacement and moment expressions from Table 1 for this boundary are written using Eq. (24) near the point $\bar{x}_0 = 0$ to arrive at Eq. (27).

$$
W_b(0) = 0, \quad W_s(0) = 0, \quad W_b(2) = 0, \quad W_s(2) = 0 \tag{27}
$$

At $\bar{x} = 1$, different boundary conditions are applicable to the SF, SS and SC plates. These are obtained from expressions in Table 1 written, again, using Eq. (24) near the point $\bar{x}_0 = 0$ to arrive at the following.

***C-type boundary*:**

$$\sum_{k=0}^{\bar{N}} W_b(k) = 0, \quad \sum_{k=0}^{\bar{N}} W_s(k) = 0, \quad \sum_{k=1}^{\bar{N}} k W_b(k) = 0, \quad \sum_{k=1}^{\bar{N}} k W_s(k) = 0 \tag{28}$$

***S-type boundary*:**

$$\sum_{k=2}^{\bar{N}} W_b(k) = 0, \quad \sum_{k=2}^{\bar{N}} W_s(k) = 0, \quad -D_{11} \sum_{k=3}^{\bar{N}} k(k-1) W_b(k) + D_{12}\beta^2 \sum_{k=1}^{\bar{N}} W_b(k) = 0, \tag{29a}$$

$$-\left(\frac{1}{84}\right)\left(D_{11} \sum_{k=3}^{\bar{N}} k(k-1) W_s(k) - D_{12}\beta^2 \sum_{k=1}^{\bar{N}} W_s(k)\right) = 0, \tag{29b}$$

***F-type boundary*:**

$$-D_{11} \sum_{k=2}^{\bar{N}} k(k-1) W_b(k) + D_{12}\beta^2 \sum_{k=1}^{\bar{N}} W_b(k) = 0, \tag{30a}$$

$$-\left(\frac{1}{84}\right)\left(D_{11} \sum_{k=2}^{\bar{N}} k(k-1) W_s(k) - D_{12}\beta^2 \sum_{k=1}^{\bar{N}} W_s(k)\right) = 0, \tag{30b}$$

$$-D_{11} \sum_{k=3}^{\bar{N}} k(k-1)(k-2) W_b(k) + \left((D_{12} + 4D_{66})\beta^2 - I_2\omega_n^2\right) \sum_{k=1}^{\bar{N}} k W_b(k) = 0 \tag{30c}$$

$$-D_{11} \sum_{k=3}^{\bar{N}} k(k-1)(k-2) W_s(k) + \left((D_{12} + 4D_{66})\beta^2 - I_2\omega_n^2 + 84A_{55}\right) \sum_{k=1}^{\bar{N}} k W_s(k) = 0 \tag{30d}$$

Since the values of the transformation terms $W_b(k)$ and $W_s(k)$ are known for $k = 0$ and 2 as given by Eq. (27), one can write the terms for $k = 1$ and 3 in terms of some unknown constants ζ and η as follows.

$$W_b(1) = \zeta_b, W_b(3) = \eta_b, W_s(1) = \zeta_s \text{ and } W_s(3) = \eta_s. \tag{31}$$

where the subscripts b and s stand for the bending and shear, respectively.

Using the recursive formulas given by Eq. (25) and values of the terms $W_b(k)$ and $W_s(k)$ for $k = 0, 1, 2, 3$ given by Eqs. (27) and (31), one can find that, $W_b(4) = 0$ and $W_s(4) = 0$. Similarly, $W_b(5)$ and $W_s(5)$ are obtained as follows.

$$W_b(5) = (c_2\zeta_b + c_3\zeta_s + 6c_1\eta_b)/120, \qquad W_s(5) = (c_6\zeta_b + c_5\zeta_s + 6c_4\eta_s)/120 \tag{32}$$

Continuing in similar manner, the subsequent terms are obtained in terms of ζ_b, η_b, ζ_s and η_s as shown in Table 2. These were evaluated up to the $\bar{N}th$ terms (i.e., $W_b(\bar{N})$ and $W_s(\bar{N})$).

Substituting the terms from $W_b(0)$ and $W_s(0)$ to $W_b(\bar{N})$ and $W_s(\bar{N})$ in Eqs. (28), (29) and (30) for the SF, SS and SC plates respectively, the following system of algebraic equations is obtained.

$$\begin{bmatrix} a_{11}\sum_{k=3}^{\bar{N}} \text{Coeff.}[W_b(k), \zeta_b] & a_{12}\sum_{k=3}^{\bar{N}} \text{Coeff.}[W_b(k), \eta_b] & a_{13}\sum_{k=3}^{\bar{N}} \text{Coeff.}[W_b(k), \zeta_s] & a_{14}\sum_{k=3}^{\bar{N}} \text{Coeff.}[W_b(k), \eta_s] \\ a_{21}\sum_{k=3}^{\bar{N}} \text{Coeff.}[W_s(k), \zeta_b] & a_{22}\sum_{k=3}^{\bar{N}} \text{Coeff.}[W_s(k), \eta_b] & a_{23}\sum_{k=3}^{\bar{N}} \text{Coeff.}[W_s(k), \zeta_s] & a_{24}\sum_{k=3}^{\bar{N}} \text{Coeff.}[W_s(k), \eta_s] \\ a_{31}\sum_{k=3}^{\bar{N}} \text{Coeff.}[W_b(k), \zeta_b] & a_{32}\sum_{k=3}^{\bar{N}} \text{Coeff.}[W_b(k), \eta_b] & a_{33}\sum_{k=3}^{\bar{N}} \text{Coeff.}[W_b(k), \zeta_s] & a_{34}\sum_{k=3}^{\bar{N}} \text{Coeff.}[W_b(k), \eta_s] \\ a_{41}\sum_{k=3}^{\bar{N}} \text{Coeff.}[W_s(k), \zeta_b] & a_{42}\sum_{k=3}^{\bar{N}} \text{Coeff.}[W_s(k), \eta_b] & a_{43}\sum_{k=3}^{\bar{N}} \text{Coeff.}[W_s(k), \zeta_s] & a_{44}\sum_{k=3}^{\bar{N}} \text{Coeff.}[W_s(k), \eta_s] \end{bmatrix} \begin{bmatrix} \zeta_b \\ \eta_b \\ \zeta_s \\ \eta_s \end{bmatrix} = \begin{bmatrix} 0 \\ 0 \\ 0 \\ 0 \end{bmatrix} \tag{33}$$

Table 2 Values of the terms $W_b\,(k)$ and $W_s\,(k)$ in the DTM formulation

k	$W_b\,(k)$	$W_s\,(k)$
0	0	0
1	ζ_b	ζ_s
2	0	0
3	η_b	η_s
4	0	0
5	$(c_2\zeta_b + c_3\zeta_s + 6c_1\eta_b)\,/120$	$(c_6\zeta_b + c_5\zeta_s + 6c_4\eta_s)\,/120$
6	0	0
7	$(c_2\eta_b + (c_1/6)\,(c_2\zeta_b + c_3\zeta_s + 6c_1\eta_b) + c_3\eta_s)\,/840$	$(c_6\eta_b + (c_4/6)\,(c_6\zeta_b + c_5\zeta_s + 6c_4\eta_s) + c_5\eta_s)\,/840$
8	0	0
9	$(c_2^2\zeta_b + c_2c_3\zeta_s + c_1^2\,(c_2\zeta_b + c_3\zeta_s) + 6c_1^3\eta_b)/362880$ $+ (6c_1\,(2c_2\eta_b + c_3\eta_s) + c_3\,(c_6\zeta_b + c_5\zeta_s + 6c_4\eta_s))\,/362880$	$(c_2c_6\zeta_b + c_5c_6\zeta_b + c_5^2\zeta_s + c_3c_6\zeta_s$ $+ 6c_1c_6\eta_b + c_4^2\,(c_6\zeta_b + c_5\zeta_s) + 6c_4^3\eta_s$ $+ 6c_4\,(c_6\eta_b + 2c_5\eta_s))/362880$
10	0	0
⋮	⋮	⋮
⋮	⋮	⋮
⋮	⋮	⋮

The summation symbol $\sum_{k=3}^{\bar{N}}\text{Coeff.}\,[W_b\,(k)\,,\zeta_b]$ used, signifies the sum of coefficients of ζ_b in the terms $W_b\,(k)\,\{k = 3, 4, \ldots, \bar{N}\}$. Definition of other elements in the matrix of Eq. (33) follows similar convention. Values of the terms a_{ij}, $\{i, j = 1, 2, 3, 4\}$ depend on the boundary condition of the plate and are given in the appendix.

Determinant of the 4×4 coefficient matrix of Eq. (33) is obtained in each case of the plate with different boundary conditions and equated to zero in order to avoid trivial solution. Solving the resulting equation(s) yields the natural frequency ω_n.

4 Taylor collocation method (TCM)

Collocation method refers to a family of various numerical solution techniques of differential equations based on selecting a candidate solution that, discretely, satisfies the governing equation and boundary conditions at certain number of domain and boundary points (collocation points), respectively. What differs between such methods is the choice of candidate solutions. The radial basis function (RBF) collocation method, for example, uses some suitable RBF centered at a given number of points. The TCM, on the other hand, makes use of Taylor polynomials derived from the Taylor series expansion of the candidate solution.

Taylor series was discovered to be useful in solving integral equations encountered in physical sciences and engineering by past researches such as [67]. The formalized approach has been presented by Kanwal and Liu [68]. Later, extension of the method to solve different kinds of differential equations and their systems has been carried out by different researchers, with the work reported in [69] as one of the early ones. Analysis of plates using this method is not very popular. However, its recent application to axisymmetric plates and shells have proved successful [70]. The concept of TCM is similar to that of DTM with the exception that the former is fully numerical while the latter is semi-analytical. In other words, contrary to the evaluation of coefficients of the Taylor series expansion by some recursive formulas in the DTM, in TCM the domain of interest needs a physical discretization followed by a collocation procedure to generate a number of algebraic equations equal to the number of the Taylor series coefficients that are finally determined by solving the system of equations so generated.

4.1 TCM formulation

The basic principle of TCM and its formulation are explained in terms of a general governing equation (of a dependent variable $w\,(x)$), over the domain Ω, described by a domain operator L subject to some generic boundary conditions, on the boundary $\Gamma\,(\mathrm{a}_0, \mathrm{a}_1)$, described by a boundary operator B as given by Eq. (34). f and g are some continuous functions of the position variable.

$$L[\![w(x)]\!] = f, \quad \text{in } \Omega \tag{34a}$$

$$B[\![w(x)]\!] = g, \quad \text{on } \Gamma \tag{34b}$$

To use the TCM, we seek a solution of Eq. (34) in the form given by Eq. (35), a Taylor series expansion of w around point c. As a priori, the function w is assumed to have nth derivatives in the interval of expansion.

$$w(x) = \sum_{n=0}^{\infty} \frac{w^{(n)}(c)}{n!} (x-c)^n, \qquad a_0 \le x, c \le a_1, \tag{35}$$

The above infinite series can be truncated at $n = \bar{N}$ (where $\bar{N}$ is chosen large enough to ensure the series convergence) as shown in Eq. (36).

$$w(x) = \sum_{n=0}^{\bar{N}} \frac{w^{(n)}(c)}{n!} (x-c)^n, \qquad a_0 \le x, c \le a_1, \tag{36}$$

To find the $\bar{N}+1$ unknowns $(w^{(n)}(c))$ in Eq. (36), the geometry of the problem is modeled by $\bar{N}+1$ randomly distributed nodes such that $\bar{N}+1 = N_d + N_b$, where N_d and N_b represent the domain and boundary nodes, respectively. Applying Eqs. (34a) and (34b) at the N_d discrete nodes in the domain and N_b nodes on the boundary, respectively, results in $\bar{N}+1$ algebraic equations as shown below.

$$L[\![w(x_i)]\!] = \sum_{n=0}^{\bar{N}} w^{(n)}(c)\, L\left[\!\!\left[\frac{1}{n!}(x_i-c)^n\right]\!\!\right], \qquad i = 1, N_d \tag{37a}$$

$$B[\![w(x_i)]\!] = \sum_{n=0}^{\bar{N}} w^{(n)}(c)\, B\left[\!\!\left[\frac{1}{n!}(x_i-c)^n\right]\!\!\right], \qquad i = 1, N_b \tag{37b}$$

Solving the above system of equations yields the values of the coefficient $w^{(n)}(c)$ for $n = 0, 1, 2, \ldots \bar{N}$. The formal procedure for the free vibration analysis based on TCM is given in the following section.

4.2 Free vibration analysis based on TCM

It can be recognized that the two fourth-order governing equations for free vibration of orthotropic plates, given by Eq. (11), can be written in the general form given by Eq. (38).

$$\sum_{k=0}^{4} \left(P_{kj} w_b^{(k)}(\bar{x}) + Q_{kj} w_s^{(k)}(\bar{x}) \right) = 0, \qquad j = 1, 2, \quad 0 \le \bar{x} \le 1 \tag{38}$$

where the coefficients P and Q are given, in terms of c_i $\{i, 1, 6\}$ (Eq. 26), thus
$P_{01} = -c_2$; $P_{21} = -c_1$; $Q_{01} = -c_3$; $Q_{02} = -c_5$; $Q_{22} = -c_4$; $P_{02} = -c_6$; $P_{41} = Q_{42} = 1$ and
$P_{kj} = Q_{kj} = 0$ for combinations of k and j otherwise.

Similarly, the general form of the eight boundary conditions (Table 1) can be written as follows.

$$\sum_{j=0}^{3} \left(\alpha_{ij} w_b^{(j)}(0) + \beta_{ij} w_b^{(j)}(1) + \gamma_{ij} w_s^{(j)}(0) + \kappa_{ij} w_s^{(j)}(1) \right) = 0, \quad i = 0, 1, 2, \ldots, 7 \tag{39}$$

The coefficients α, β, γ and κ in Eq. (39) depend on the actual boundary condition thus.

i. At $\bar{x} = 0$, $\beta_{ij} = \kappa_{ij} = 0$ for all i and j while α and γ are common for SC,SS and SF plate types as given below.

$$\alpha_{00} = \gamma_{10} = 1; \quad \alpha_{22} = -D_{11}, \alpha_{20} = D_{12}\beta^2; \quad \gamma_{32} = -\left(\frac{1}{84}\right)(D_{11}); \quad \gamma_{30} = (1/84)\, D_{12}\beta^2$$

$\alpha_{ij} = \gamma_{ij} = 0$, for combinations of i and j otherwise.

ii. At $\bar{x} = 1$, $\alpha_{ij} = \gamma_{ij} = 0$ for all i and j, while β and κ are given, depending on the fixity condition, as follows.

***C-type boundary*:**

$$\beta_{40} = \kappa_{50} = \beta_{61} = \kappa_{71} = 1$$

$\beta_{ij} = \kappa_{ij} = 0$, for combinations of i and j otherwise.

***S-type boundary*:**

$$\beta_{40} = \kappa_{50} = 1; \quad \beta_{62} = -D_{11}; \quad \beta_{60} = D_{12}\beta^2; \quad \kappa_{72} = -\left(\frac{1}{84}\right)(D_{11}); \quad \kappa_{70} = (1/84)\, D_{12}\beta^2$$

$\beta_{ij} = \kappa_{ij} = 0$, for combinations of i and j otherwise.

***F-type boundary*:**

$$\beta_{42} = \beta_{63} = \kappa_{73} = -D_{11}; \quad \beta_{40} = D_{12}\beta^2; \quad \kappa_{52} = -\left(\frac{1}{84}\right)(D_{11}); \quad \kappa_{50} = \left(\frac{1}{84}\right) D_{12}\beta^2;$$

$$\beta_{61} = \left((D_{12} + 4D_{66})\,\beta^2 - I_2\omega_n^2\right); \quad \kappa_{71} = \left((D_{12} + 4D_{66})\,\beta^2 - I_2\omega_n^2 + 84A_{55}\right)$$

$$\beta_{ij} = \kappa_{ij} = 0, \text{ for combinations } of\ i \text{ and } j \text{ otherwise.}$$

Equation (40) gives the approximate solutions for the bending and shear components of the transverse displacement, written as two truncated Taylor series expansions around $\bar{c}$ in each case. $\bar{N}$ is selected large enough to ensure the series convergence.

$$w_b(x) = \sum_{n=0}^{\bar{N}} \frac{w_b^{(n)}(\bar{c})}{n!}(\bar{x} - \bar{c})^n, \qquad 0 \le \bar{x}, \bar{c} \le 1, \quad N \ge 3 \tag{40a}$$

$$w_s(x) = \sum_{n=0}^{\bar{N}} \frac{w_s^{(n)}(\bar{c})}{n!}(\bar{x} - \bar{c})^n, \qquad 0 \le \bar{x}, \bar{c} \le 1, \quad N \ge 3 \tag{40b}$$

A set of $\bar{x}_i$, $\left(i = 0, 1, 2, \ldots, \bar{N}\right)$ collocation points at some specified intervals within the problem domain is used in order to find the unknown Taylor coefficients $w_b^{(n)}(\bar{c})$ and $w_s^{(n)}(\bar{c})$ $\left\{n = 0, 1, 2, \ldots \bar{N}\right\}$. However, because there are two boundary conditions at each of the two boundary nodes, this will result in two extra equations more than the number of unknowns. Therefore, the present work chooses to create two more virtual nodes outside the domain, one adjacent to each of the boundary nodes at a distance $d\bar{x}$. Consequently, the following range for $\bar{x}_i$ results.

$$-d\bar{x} = \bar{x}_0 < \bar{x}_1 < \cdots \bar{x}_{N-1} < \bar{x}_N = 1 + d\bar{x}$$

where, for a uniform interval, the value of $\bar{x}_i$ becomes

$$\bar{x}_i = -\mathrm{d}\bar{x} + i\frac{1 + 2\mathrm{d}\bar{x}}{\bar{N}}, i = 0, 1, 2, \ldots \bar{N} \tag{41}$$

Writing Eq. (40) in terms of matrices, one obtains.

$$w_b(\bar{x}) = \bar{X} M_0 A_b \tag{42a}$$

$$w_s(\bar{x}) = \bar{X} M_0 A_s \tag{42b}$$

where

$$\bar{X} = \left[1 \;\; (\bar{x} - \bar{c}) \;\; (\bar{x} - \bar{c})^2 \;\; \cdots \;\; (\bar{x} - \bar{c})^{\bar{N}}\right]$$

$$M_0 = \begin{bmatrix} \frac{1}{0!} & 0 & 0 & \cdots & 0 \\ 0 & \frac{1}{1!} & 0 & \cdots & 0 \\ 0 & 0 & \frac{1}{2!} & \cdots & 0 \\ \vdots & \vdots & \vdots & \vdots & \vdots \\ 0 & 0 & 0 & \cdots & \frac{1}{\bar{N}!} \end{bmatrix}$$

$$A_b = \left[W_b^{(0)}(\bar{c})\ W_b^{(1)}(\bar{c})\ W_b^{(2)}(\bar{c}) \cdots W_b^{(\bar{N})}(\bar{c}) \right]^T$$
$$A_s = \left[W_s^{(0)}(\bar{c})\ W_s^{(1)}(\bar{c})\ W_s^{(2)}(\bar{c}) \cdots W_s^{(\bar{N})}(\bar{c}) \right]^T$$

Applying Eq. (42) at $\bar{x}_i$ collocation points yields

$$w_b(\bar{x}_i) = \bar{X}_i M_0 A_b \qquad i = 0, 1, 2, \ldots, \bar{N} \tag{43a}$$
$$w_s(\bar{x}_i) = \bar{X}_i M_0 A_s \qquad i = 0, 1, 2, \ldots, \bar{N} \tag{43b}$$

where

$$\bar{X}_i = \left[1\ (\bar{x}_i - \bar{c})\ (\bar{x}_i - \bar{c})^2 \cdots (\bar{x}_i - \bar{c})^{\bar{N}} \right]$$

The vector of zero derivatives of the solution can be denoted as follows

$$w_b^{(0)} = \left[w_b(\bar{x}_0)\, w_b(\bar{x}_1)\ w_b(\bar{x}_2) \cdots w_b\left(\bar{x}_{\bar{N}}\right) \right]^T,$$
$$w_s^{(0)} = \left[w_s(\bar{x}_0)\, w_s(\bar{x}_1)\ w_s(\bar{x}_2) \cdots w_s\left(\bar{x}_{\bar{N}}\right) \right]^T$$

Hence, Eq. (43) can be written in the form shown below.

$$w_b^{(0)} = C M_0 A_b \tag{44a}$$
$$w_s^{(0)} = C M_0 A_s \tag{44b}$$

where

$$C = \left[\bar{X}_0\, \bar{X}_1 \cdots \bar{X}_{\bar{N}} \right]^T = \begin{bmatrix} 1 & (\bar{x}_0 - \bar{c}) & (\bar{x}_0 - \bar{c})^2 & \cdots & (\bar{x}_0 - \bar{c})^{\bar{N}} \\ 1 & (\bar{x}_1 - \bar{c}) & (\bar{x}_1 - \bar{c})^2 & \cdots & (\bar{x}_1 - \bar{c})^{\bar{N}} \\ \vdots & \vdots & \vdots & \cdots & \vdots \\ 1 & \left(\bar{x}_{\bar{N}} - \bar{c}\right) & \left(\bar{x}_{\bar{N}} - \bar{c}\right)^2 & \cdots & \left(\bar{x}_{\bar{N}} - \bar{c}\right)^{\bar{N}} \end{bmatrix}$$

Similarly, the vector of the derivatives becomes

$$w_b^{(k)} = C M_k A_b \tag{45a}$$
$$w_s^{(k)} = C M_k A_s \tag{45b}$$

where

$$w_b^{(k)} = \left[w_b^{(k)}(\bar{x}_0)\ w_b^{(k)}(\bar{x}_1)\ w_b^{(k)}(\bar{x}_2) \cdots w_b^{(k)}\left(\bar{x}_{\bar{N}}\right) \right]^T,$$
$$w_s^{(k)} = \left[w_s^{(k)}(\bar{x}_0)\ w_s^{(k)}(\bar{x}_1)\ w_s^{(k)}(\bar{x}_2) \cdots w_s^{(k)}\left(\bar{x}_{\bar{N}}\right) \right]^T$$

Applying Eq. (38) at the discrete interior points ($i = 1, 2, \ldots, \bar{N} - 1$) yields

$$\sum_{k=0}^{4} \left(P_{kj} w_b^{(k)}(\bar{x}_i) + Q_{kj} w_s^{(k)}(\bar{x}_i) \right) = 0, \quad j = 1, 2, \tag{46}$$

or, equivalently

$$\sum_{k=0}^{4} \left(P_{kj} w_b^{(k)} + Q_{kj} w_s^{(k)} \right) = 0, \quad j = 1, 2, \tag{47}$$

Substituting Eq. (45) in Eq. (47) yields

$$\left[\sum_{k=0}^{4} P_{kj} C M_k \right] A_b + \left[\sum_{k=0}^{4} Q_{kj} C M_k \right] A_s = [0], \qquad j = 1, 2, \quad 0 \le \bar{x} \le 1 \tag{48}$$

Since the system of equations given by Eq. (48) is a consequence of collocating over the interior nodes to satisfy Eq. (38), it therefore represents a set of $\left(\bar{N}-i\right)$ equations involving $\left(\bar{N}+1\right)$ unknowns. Hence, the remaining $(i+1)$ equations are generated as given in Eq. [49] by considering the boundary conditions given by Eq. (39).

$$\left[\sum_{j=0}^{3}\left(\alpha_{ij}X_0M_j+\beta_{ij}X_{\bar{N}}M_j\right)\right]A_b+\left[\sum_{j=0}^{3}\left(\gamma_{ij}X_0M_j+\kappa_{ij}X_{\bar{N}}M_j\right)\right]A_s=[0] \tag{49}$$

The overall set of the system of equations required to solve for the vector $\mathrm{A}=[A_b,A_s]^T$ of the unknown coefficients is given by Eq. (50) as a combination of domain and boundary equations.

$$\begin{bmatrix}\left[\sum_{k=0}^{4}P_{kj}CM_k\right] & \left[\sum_{k=0}^{4}Q_{kj}CM_k\right]\\ \left[\sum_{j=0}^{3}\left(\alpha_{ij}X_0M_j+\beta_{ij}X_{\bar{N}}M_j\right)\right] & \left[\sum_{j=0}^{3}\left(\gamma_{ij}X_0M_j+\kappa_{ij}X_{\bar{N}}M_j\right)\right]\end{bmatrix}\begin{bmatrix}A_b\\ A_s\end{bmatrix}=\begin{bmatrix}0\\ 0\end{bmatrix}, \tag{50}$$

The natural frequency parameters $\bar{\omega}_n$ are obtained by equating determinant of the $2\left(\bar{N}+1\right)\times 2\left(\bar{N}+1\right)$ coefficient matrix of Eq. (50) to zero and solving the resulting equation.

5 Results and discussion

By implementing the DTM and TCM formulations presented in the previous sections, results for free vibration analysis of orthotropic rectangular plate, based on the present theory (the RPT), with boundary conditions as given in Table 1 are presented in the first part of the present section.

Comparison of the predicted results with those of other theories is, first, illustrated in Sect. 5.1 for orthotropic plates whose exact solution is available in the literature. Section 5.2 presents an extension of the problem to cover SF, SC and SS rectangular plates. Convergence study for both DTM and TCM is given in Sect. 5.2.1, followed by a parametric study, in Sect. 5.2.2, to illustrate the effect of different values of the thickness ratio (a/h), the aspect ratio (a/b) and the modular ratio (E_1/E_2). For the sake of verification, analytical results reported in [35] are given in each case.

Results for some cases whose analytical solutions are not readily available, particularly based on the two-variable refined plate theory, are presented in Sect. 5.2.3. Formulations of three more plate theories, the CPT, the FSDT [10,60,61] and the HSDT [62], were implemented and solved using both the DTM and TCM for verification purposes. Similar to the case of RPT presented in the present work, the high-order theory in [62] considers both the displacements in x and y directions, u and v, respectively, to be composed of shear and bending components. However, while the bending components in [62] are similar to that of CPT, the shear components are assumed to be exponential in nature with respect to the thickness coordinate. For that reason, their theory is also referred to as the exponential shear deformation theory.

5.1 RPT-based DTM and TCM versus other plate theories

In order to demonstrate the performance of DTM and TCM based on the RPT, a simply supported square orthotropic plate made from same material as that reported in the reference of Reddy [17] and, later, adopted in [30,35], is considered. The material properties are $E_1=20,830ksi$, $E_2=10,940ksi$, $G_{12}=6,100ksi$, $G_{13}=3,710ksi$, $\upsilon_{12}=0.44$ and $\upsilon_{21}=0.23$.

Three more plate theories, namely CPT, FSDT [10,60,61] and HSDT [62], were also formulated, implemented and solved using both the DTM and TCM in order to demonstrate differences between models and advantages of the proposed analysis. Details of the governing equations of these theories can be found in the respective mentioned references.

As shown in Table 3, natural frequency parameters $\bar{\omega}_n=\omega_n h\sqrt{\rho/Q_{11}}$ predicted by DTM and TCM based on the present theory compare favorably with the exact solution [71] based on 3D elasticity theory and the HSDT [62] with a maximum deviation from the exact solution of 0.67 % (on the conservative side). However, it can be noticed that, while the CPT overestimates the natural frequencies, the FSDT results are a little less

Table 3 Natural frequency parameters $\bar{\omega}_n = \omega_n h\sqrt{\rho/Q_{11}}$ of simply supported square plate with $\frac{a}{h} = 10$

Mode	Exact $\bar{\omega}_n$ [59]	Present	CPT		FSDT		HSDT		RPT	
			$\bar{N}$	$\bar{\omega}_n$	$\bar{N}$	$\bar{\omega}_n$	$\bar{N}$	$\bar{\omega}_n$	$\bar{N}$	$\bar{\omega}_n$
1	0.0474	DTM	7	0.0532	7	0.0489	6	0.0439	7	0.0512
			9	0.0490	9	0.0473	8	0.0492	9	0.0474
			11	0.0493	11	0.0474	10	0.0474	11	0.0477
			12	0.0493	12	0.0474	11	0.0474	12	0.0477
		Error (%)		4.01		0.00		0.00		0.63
		TCM	4	0.0484	2	1.3161	5	0.4623	4	0.0458
			5	0.0485	4	0.0468	7	0.0473	6	0.0469
			6	0.0493	6	0.0474	9	0.0474	8	0.0477
			7	0.0493	7	0.0474	10	0.0474	9	0.0477
		Error (%)		4.01		0.00		0.00		0.63
2	0.1033	DTM	7	0.1114	6	0.1015	8	0.1195	7	0.1054
			9	0.1097	8	0.1021	10	0.1185	9	0.1039
			11	0.1098	10	0.1032	12	0.1033	11	0.1040
			12	0.1098	11	0.1032	13	0.1033	12	0.1040
		Error (%)		6.29		−0.10		0.00		0.68
		TCM	4	0.1085	7	0.1051	10	0.1085	4	0.1028
			5	0.1094	9	0.1031	12	0.1015	5	0.1036
			6	0.1098	11	0.1032	14	0.1033	6	0.1040
			7	0.1098	12	0.1032	15	0.1033	7	0.1040
		Error (%)		6.29		−0.10		0.00		0.68
3	0.1888	DTM	5	0.2030	11	0.1843	7	0.2354	5	0.1866
			7	0.2082	13	0.1867	9	0.2178	7	0.1907
			9	0.2070	15	0.1884	11	0.1887	9	0.1898
			10	0.2070	16	0.1884	12	0.1887	10	0.1898
		Error (%)		9.64		−0.21		−0.05		0.53
		TCM	4	0.2060	10	0.1861	9	0.1886	4	0.1890
			5	0.2068	12	0.1887	11	0.1887	6	0.1899
			6	0.2071	14	0.1884	13	0.1887	8	0.1898
			7	0.2071	15	0.1884	14	0.1887	9	0.1898
		Error (%)		9.69		−0.21		−0.05		0.53
4	0.2969	DTM	5	0.3335	8	0.2986	7	0.3467	7	0.2986
			7	0.3382	10	0.2924	9	0.3318	9	0.2979
			9	0.3372	12	0.2960	11	0.2970	11	0.2980
			10	0.3372	13	0.2960	12	0.2970	12	0.2980
		Error (%)		13.57		−0.30		0.03		0.37
		TCM	4	0.3363	13	0.2992	17	0.2967	4	0.2973
			5	0.3370	15	0.2956	19	0.2964	5	0.2978
			6	0.3372	17	0.2960	21	0.2965	6	0.2980
			7	0.3372	18	0.2960	22	0.2965	7	0.2980
		Error (%)		13.57		−0.30		−0.13		0.37

conservative compared to the present theory, at least for the orthotropic plate considered here. Although so far there is no available plate theory that is both as simple as the CPT and as accurate (in all cases) as the other more complex higher-order theories, the RPT attempts to satisfy such qualities to some extents. For instance, its formulation resembles that of the CPT and, once the shear terms are dropped, the governing equations (Eq. 11) of the RPT turn, exactly, to the equation of CPT. Second, the elimination for the need of shear correction as required in some shear deformation theories gives the present theory an additional advantage because it still satisfies the zero-traction boundary condition at the top and bottom surfaces of the plate. In addition, the resulting system of equations are easier to solve than those of other higher-order theories.

With regard to the method of solution, the results shown in Table 3 based on DTM and TCM agree perfectly with those reported in Refs. [30,35]. However, while both the DTM and TCM require lower $\bar{N}$ value to achieve convergence for all the four modes based on RPT, the $\bar{N}$ value needed in the FSDT and HSDT solution increases with increase in the mode and becomes much higher than those needed in RPT. This is not surprising considering the complexity of the governing equations of FSDT and HSDT (available in the respective references) compared to those of RPT (Eq. 11) and CPT.

By extending the analysis to cover additional plate types in terms of boundary conditions, geometric dimensions and modular ratios, numerical results in the subsequent subsections are used to elaborate more on the capability of the two methods of solution (DTM and TCM) proposed in this research.

5.2 Extension to general rectangular plates with different boundary conditions

In this section, consideration is, initially, given to SF, SS and SC orthotropic plates having generic rectangular shapes with various thickness ratios. Non-dimensionalized material properties [35,72] are assumed thus: $G_{12}/E_2 = G_{13}/E_2 = 0.5, G_{23}/E_2 = 0.2, \upsilon_{12} = 0.25$ and E_1/E_2 is varied. First, convergence studies for the DTM and TCM are carried out, followed by parametric studies. Next, multi-span plates and plates with stepped thickness and end rotational springs are considered.

5.2.1 Convergence studies

In order to demonstrate the convergence behavior of DTM and TCM applied to SF, SS and SC plates, nine cases of rectangular orthotropic plates are considered for each of SF, SS and SC plates, resulting in a total of 27 cases. The convergence results for the fundamental natural frequency parameters $\bar{\omega} = \omega \frac{a^2}{h}\sqrt{\rho/E_2}$ illustrating effects of the aspect ratio, thickness ratio and modular ratio are, respectively, presented in Tables 4, 5 and 6. Results predicted based on CPT and the analytical solution reported in [35] are also shown. Good agreement exists between the DTM, TCM and analytical results, with the TCM resulting in lower percentage errors almost consistently. However, it should be noted that, based on the CPT, both DTM and TCM provide solutions having the same accuracy. In terms of computational demand, more computer memory is needed in TCM since a system matrix of size $2\left(\bar{N}+1\right) \times 2\left(\bar{N}+1\right)$ needs to be handled, while DTM formulation results in only a 4×4 matrix size and, hence, it is less resource-consuming.

The purpose of using different values of a/h is to demonstrate the effect of plate thickness on the result. It is evident, from Table 5, that the magnitude of the error in CPT is higher for lower thickness ratios $a/h = 5$ and 20 (i.e., thick plates). This is expected due to the fact that CPT formulation neglects the effect of shear which, on the other hand, is taken care of in RPT. Shear effects are only negligible in case of thin plates, and consequently, the error in the plates with higher values of a/h (such as 100) becomes negligible in the predictions by CPT.

Increase in the modular ratio also causes increase in the shear effect, particularly for the SS and SC plates. That is why, as given in Table 6, error in the solution based on CPT also increases with increase in E_1/E_2. Such effect is, however, not observed in the SF plate because the free end relaxes the stiffness of the plate which, in turn, causes less shear effect.

5.2.2 Parametric studies

Apart from the 27 cases analyzed in Sect. 5.2.1 above, a comprehensive parametric study consisting of 45 cases with variations in the material modular ratio and geometric ratios is carried out for each of the SF, SS and SC plate types. Hence, a total of 135 cases with the DTM and TCM applied to obtain solutions are presented. The end results of the fundamental natural frequency parameters $\bar{\omega} = \omega \frac{a^2}{h}\sqrt{\rho/E_2}$ are presented in Tables 7, 8 and 9 for the SF, SS and SC plates, respectively. Variables targeted for the parametric study comprise of different values of the thickness ratio (a/h), the aspect ratio (a/b) and the modular ratio (E_1/E_2). These results cover other ranges of the variables not covered in Sect. 5.2.1, and they are presented in a more definite pattern to enhance understanding the obvious roles played by each of the variables. Value of $\bar{N}$ used in each method is indicated as well as the error computed with respect to the analytical results available in [35].

It can be noticed that, throughout the results presented in Tables 7, 8 and 9, the effect of increasing the aspect ratio and thickness ratio is to cause a corresponding increase in the fundamental natural frequency parameter, hence, increase in the fundamental natural frequency for all the plate types studied. Similarly, the effect of increasing the modular ratio causes an increase in the fundamental natural frequency parameter for the SS and SC plates. On the other hand, no such effect is observed in the case of SF plate because of its free end which lowers the plate's stiffness. Denoting the fundamental natural frequency parameters for the SF, SS and SC plates as $\bar{\omega}_{SF}$, $\bar{\omega}_{SS}$ and $\bar{\omega}_{SC}$, respectively, it can be seen that effect of end fixity suggests that, under the same condition (same thickness ratio, aspect ratio and modular ratio), values of the fundamental natural frequency parameters have magnitudes in the order $\bar{\omega}_{SC} > \bar{\omega}_{SS} > \bar{\omega}_{SF}$. This is also confirmed by a general analysis performed for arbitrary geometry and for elastic stiffeners along the part of the boundary in [73]. It is logical to have such behavior due to the fact that increase in fixity results in higher reactive effects, in form of increase in the stiffness, thereby amplifying the natural frequency.

It is worth mentioning that the both the two numerical methods, DTM and TCM, adopted in obtaining these solutions do not require iterations as is the case with the analytical results reported in [35]. Additionally, unlike other element-based numerical techniques, the DTM and TCM can be used to present solutions in symbolic

Table 4 Convergence of fundamental frequency parameters $\bar{\omega} = \omega \frac{a^2}{h}\sqrt{\rho/E_2}$ for plates with $\frac{a}{h} = 50$ and $\frac{E_1}{E_2} = 10$

a/b	Theory/method		SF		SS		SC	
			$\bar{N}$	$\bar{\omega}$	$\bar{N}$	$\bar{\omega}$	$\bar{N}$	$\bar{\omega}$
0.5	CPT			1.3189		9.3409		14.3417
		Error (%)		0.02		0.39		0.87
	Present	DTM	7	1.3215	7	11.6660	7	13.8004
			9	1.3188	9	9.1326	9	13.7184
			11	1.3187	11	9.3230	11	14.3240
			12	1.3187	12	9.3230	12	14.3240
		Error (%)		0.01		0.20		0.75
		TCM	5	1.3251	6	9.3454	20	14.2192
			7	1.3188	8	9.3035	22	14.2190
			9	1.3186	10	9.3044	24	14.2188
			10	1.3186	11	9.3044	25	14.2188
		Error (%)		0.00		0.00		0.01
	Analytical			1.3186		9.3044		14.2179
1.0	CPT			3.6107		10.4928		15.1988
		Error (%)		0.10		0.38		0.77
	Present	DTM	7	3.6280	7	12.9848	7	14.1354
			9	3.6091	9	10.3015	9	14.6449
			11	3.6077	11	10.4680	11	15.1745
			12	3.6077	12	10.4680	12	15.1745
		Error (%)		0.01		0.14		0.61
		TCM	13	3.6074	6	10.4893	20	15.0833
			15	3.6073	8	10.4522	22	15.0832
			17	3.6072	10	10.4530	24	15.0830
			18	3.6072	11	10.4530	25	15.0830
		Error (%)		0.00		0.00		0.00
	Analytical			3.6072		10.4530		15.0824
2.0	CPT			12.2293		17.1223		20.5766
		Error (%)		0.39		0.55		0.77
	Present	DTM	7	12.3176	7	18.3751	7	20.0321
			9	12.2106	9	16.9400	9	20.2020
			11	12.1851	11	17.0360	11	20.4814
			12	12.1851	12	17.0360	12	20.4814
		Error (%)		0.03		0.04		0.30
		TCM	23	12.1822	6	17.0511	20	20.4202
			25	12.1821	8	17.0289	22	20.4201
			27	12.1817	10	17.0294	24	20.4200
			28	12.1817	11	17.0294	25	20.4200
		Error (%)		0.00		0.00		0.00
	Analytical			12.1817		17.0294		20.4196

form which warrants the possibility of obtaining other secondary variables by differentiation, integration, etc. Also, the obvious advantage of eliminating the need for method calibration as required in other meshless methods, such as the Kansa method and method of fundamental solutions, adds to the appealing nature of the presented methods.

5.2.3 Multi-span plates and plates with stepped thickness and end rotational springs

Since the problems presented in Sects. 5.2.1 and 5.2.2 are for single-span plates analyzed by the proposed methods and verified using an existing analytical solution, the present section aims at presenting results for some cases whose analytical solution is not readily available particularly based on the two-variable refined plate theory. For the sake of verification, formulation of three more plate theories, the CPT, the FSDT [10,60,61] and the HSDT [62], was implemented and solved using both the DTM and TCM. These are the same plate theories against which comparison of the results in Sect. 5.2.1 was made.

The analysis starts by, firstly, considering a multi-span Levy plate, consisting of $(n-1)$ internal supports. Various engineering applications of such plates exist, such as in bridge decks, floor slabs, aeroplane parts, etc. Such problems can be, conveniently, modeled as plates with internal line supports are shown in Fig. 2. The problem now goes beyond just satisfying the governing equations in a span and the external boundary conditions as is the case in the analysis carried out in the previous sections. In this case, the governing equations must be satisfied

Table 5 Convergence of fundamental frequency parameters $\bar{\omega} = \omega \frac{a^2}{h}\sqrt{\rho/E_2}$ for plates with $\frac{a}{b} = 2.0$ and $\frac{E_1}{E_2} = 10$

a/h	Theory/method		SF		SS		SC	
			$\bar{N}$	$\bar{\omega}$	$\bar{N}$	$\bar{\omega}$	$\bar{N}$	$\bar{\omega}$
5	CPT			9.9516		15.8800		19.0438
		Error (%)		10.91		36.43		48.79
	Present	DTM	32	8.9852	11	11.6428	33	12.8088
			34	8.9821	13	11.6392	35	12.8056
			36	8.9755	15	11.6394	37	12.8035
			37	8.9755	16	11.6394	38	12.8035
		Error (%)		0.03		0.00		0.03
		TCM	20	8.9732	6	11.6474	18	12.7992
			22	8.9728	8	11.6392	20	12.7991
			24	8.9727	10	11.6394	22	12.7991
			25	8.9727	11	11.6394	23	12.7991
		Error (%)		0.00		0.00		0.00
	Analytical			8.9727		11.6394		12.7991
20	CPT			12.1844		17.0490		20.4859
		Error (%)		2.38		3.31		4.63
	Present	DTM	9	11.9539	9	16.4206	11	19.6737
			11	11.9308	11	16.5114	13	19.6145
			13	11.9240	13	16.5010	15	19.4740
			14	11.9240	14	16.5010	16	19.4740
		Error (%)		0.19		−0.01		−0.54
		TCM	20	11.9033	6	16.5230	14	19.5838
			22	11.9029	8	16.5026	16	19.5827
			24	11.9030	10	16.5031	18	19.5820
			25	11.9030	11	16.5031	19	19.5820
		Error (%)		0.02		0.00		0.01
	Analytical			11.9012		16.5030		19.5797
100	CPT			12.2357		17.1329		20.5897
		Error (%)		0.10		0.14		0.19
	Present	DTM	5	12.6318	7	18.4801	5	21.5602
			7	12.3307	9	17.0179	7	21.2473
			9	12.2221	11	17.1030	9	20.3215
			10	12.2221	12	17.1030	10	20.3215
		Error (%)		−0.01		−0.04		−1.11
		TCM	9	12.2246	6	17.1315	4	19.7242
			11	12.2241	8	17.1089	6	20.5622
			13	12.2240	10	17.1094	8	20.5500
			14	12.2240	11	17.1094	9	20.5500
		Error (%)		0.00		0.00		0.00
	Analytical			12.2238		17.1094		20.5500

in each of the "n" spans in turn. Also, in addition to the boundary conditions given in Table 1, the compatibility conditions given by Eqs. (51) to (58) must hold at the interface between the ith and $(i+1)$th span in order to ensure continuity at the location of the internal supports. Consequently, the system of equations that needs to be handled becomes different and much more involving than the case of single-span plates earlier analyzed.

$$(w_b)_i = 0 \tag{51}$$

$$(w_s)_i = 0 \tag{52}$$

$$(w_b)_{i+1} = 0 \tag{53}$$

$$(w_s)_{i+1} = 0 \tag{54}$$

$$\left(w_b'\right)_i = \left(w_b'\right)_{i+1} \tag{55}$$

$$\left(w_s'\right)_i = \left(w_s'\right)_{i+1} \tag{56}$$

$$\left(-D_{11}w_b'' + D_{12}\beta^2 w_b\right)_i = \left(-D_{11}w_b'' + D_{12}\beta^2 w_b\right)_{i+1} \tag{57}$$

$$\left(-(1/84)\left(D_{11}w_s'' - D_{12}\beta^2 w_s\right)\right)_i = \left(-(1/84)\left(D_{11}w_s'' - D_{12}\beta^2 w_s\right)\right)_{i+1} \tag{58}$$

Table 6 Convergence of fundamental frequency parameters $\bar{\omega} = \omega \frac{a^2}{h}\sqrt{\rho/E_2}$ for plates with $\frac{a}{b} = 0.5$ and $\frac{a}{h} = 100$

$\frac{E_1}{E_2}$	Theory/method		SF		SS		SC	
			$\bar{N}$	$\bar{\omega}$	$\bar{N}$	$\bar{\omega}$	$\bar{N}$	$\bar{\omega}$
10	CPT			1.3190		9.3416		14.3442
		Error (%)		0.00		0.09		0.21
	Present	DTM	5	1.3407	7	8.5354	7	13.2488
			7	1.3217	9	9.1572	9	13.7818
			9	1.3190	11	9.3220	11	14.3220
			10	1.3190	12	9.3220	12	14.3220
		Error (%)		0.00		−0.12		0.06
		TCM	4	1.4772	8	9.3317	20	14.3133
			5	1.3253	10	9.3327	22	14.3132
			7	1.3190	12	9.3326	24	14.3131
			8	1.3190	13	9.3326	25	14.3131
		Error (%)		0.00		−0.01		0.00
	Analytical			1.3190		9.3331		14.3137
25	CPT			1.3193		14.4571		22.4246
		Error (%)		0.01		0.23		0.53
	Present	DTM	5	1.3281	7	18.0748	7	21.0018
			7	1.3202	9	14.1457	9	21.4772
			9	1.3192	11	14.4450	11	22.4400
			10	1.3192	12	14.4450	12	22.4400
		Error (%)		0.00		0.14		0.60
		TCM	4	1.4711	6	14.4902	16	22.3075
			6	1.3197	8	14.4223	18	22.3072
			8	1.3192	10	14.4238	20	22.3069
			9	1.3192	11	14.4238	21	22.3069
		Error (%)		0.00		0.00		0.00
	Analytical			1.3192		14.4245		22.3069
40	CPT			1.3193		18.1866		28.2839
		Error (%)		0.00		0.36		0.84
	Present	DTM	5	1.3249	7	22.7126	7	26.7612
			7	1.3199	9	17.7683	9	27.0147
			9	1.3193	11	18.1570	11	28.2620
			10	1.3193	12	18.1570	12	28.2620
		Error (%)		0.00		0.20		0.76
		TCM	4	1.4696	8	18.1187	18	28.0500
			5	1.3210	10	18.1206	20	28.0490
			7	1.3193	12	18.1205	22	28.0480
			8	1.3193	13	18.1205	23	28.0480
		Error (%)		0.00		−0.01		0.00
	Analytical			1.3193		18.1215		28.0480

The two proposed methods, DTM and TCM, have been implemented based on RPT to solve a three-span plate problem with each span having a square shape. The same problem was also solved based on three more plate theories (CPT, FSDT and HSDT) using the two techniques (DTM and TCM), and the results are shown in Table 10.

In order to generalize the case of multi-span Levy plates, plates with end rotational springs at the two external boundaries (at $x = 0$ and $x = a$ or, in non-dimensionalized form, $\bar{x} = 0$ and $\bar{x} = 1$) are considered. The springs can represent location of continuity with adjacent plate members whose analysis is not included. However, more interestingly, elastically supported plates represent the most general scenario of boundary condition. The springs with non-dimensional stiffness $\bar{k}_s = k_s/\left(a^2 E_2\right)$ are used to model the two-span plate shown in Fig. 3. k_s is the actual stiffness constant of the spring. Results achieved using the presented techniques in this work for $\delta = 0.3$ are shown in Table 11 based on both RPT and other plate theories.

The approach of formulating the multi-span problem above can be extended to deal with Levy plates with stepped thickness which can have any number of thickness segments "n." Again, for the sake of generalization of the edge fixity conditions, end rotational springs are incorporated in the model as shown in Fig. 4. Although the problem consists of a single span, the presence of the thickness steps results in the need to ensure continuity conditions at the interface between the segments by satisfying the additional equations given by Eqs. (59) to (66). These conditions are different from those (Eqs. 51–58) satisfied in the case of multi-span plates. Results for a plate with two thickness steps of equal length in x-direction are shown in Table 11. It should be noted that, unlike the previous cases treated for SS, SC and SF plates, and unlike the multi-span plates without springs,

Table 7 Fundamental frequency parameters $\bar{\omega} = \omega \frac{a^2}{h}\sqrt{\rho/E_2}$ for SF plate

a/b	a/h	Method		$\bar{N}$	E_1/E_2									
					3		20		30		40		50	
0.5	5	Present	DTM/%Err.	20	1.2808	0.23	1.2801	0.14	1.2797	0.09	1.2794	0.07	1.2792	0.05
			TCM/%Err.	25	1.2780	0.01	1.2783	0.00	1.2785	0.00	1.2785	0.00	1.2786	0.00
		Analytical		–	1.2779		1.2783		1.2785		1.2785		1.2786	
	20	Present	DTM/%Err.	22	1.3164	0.03	1.3165	0.00	1.3166	0.00	1.3168	0.02	1.3169	0.02
			TCM/%Err.	25	1.3161	0.01	1.3165	0.00	1.3166	0.00	1.3167	0.01	1.3167	0.00
		Analytical		–	1.3160		1.3165		1.3166		1.3166		1.3167	
	50	Present	DTM/%Err.	10	1.3189	0.05	1.3189	0.01	1.3190	0.01	1.3190	0.01	1.3190	0.01
			TCM/%Err.	15	1.3183	0.00	1.3188	0.00	1.3189	0.00	1.3189	0.00	1.3190	0.01
		Analytical		–	1.3183		1.3188		1.3189		1.3189		1.3189	
1.0	5	Present	DTM/%Err.	31	3.2680	0.21	3.2582	0.00	3.2587	0.00	3.2589	0.00	3.2591	0.00
			TCM/%Err.	25	3.2610	0.00	3.2582	0.00	3.2586	0.00	3.2589	0.00	3.2591	0.00
		Analytical		–	3.2611		3.2582		3.2586		3.2589		3.2591	
	20	Present	DTM/%Err.	16	3.5949	0.14	3.5875	0.06	3.5874	0.05	3.5876	0.05	3.5877	0.05
			TCM/%Err.	25	3.5900	0.00	3.5855	0.00	3.5857	0.00	3.5859	0.00	3.5860	0.00
		Analytical		–	3.5900		3.5854		3.5857		3.5858		3.5859	
	50	Present	DTM/%Err.	12	3.6309	0.52	3.6080	0.02	3.6082	0.01	3.6084	0.01	3.6085	0.01
			TCM/%Err.	15	3.6122	0.00	3.6075	0.00	3.6078	0.00	3.6080	0.00	3.6081	0.00
		Analytical		–	3.6121		3.6074		3.6077		3.6079		3.6080	
2.0	5	Present	DTM/%Err.	31	9.0750	0.88	8.9739	0.03	8.9726	0.00	8.9730	0.00	8.9737	0.00
			TCM/%Err.	25	8.9967	0.01	8.9715	0.00	8.9722	0.00	8.9730	0.00	8.9737	0.00
		Analytical		–	8.9954		8.9715		8.9722		8.9730		8.9737	
	20	Present	DTM/%Err.	20	12.0400	0.73	11.9100	0.12	11.9000	0.05	11.9000	0.05	11.9050	0.09
			TCM/%Err.	25	11.9551	0.02	11.8960	0.01	11.8949	0.00	11.8947	0.00	11.8947	0.00
		Analytical		–	11.9528		11.8952		11.8945		11.8944		11.8946	
	50	Present	DTM/%Err.	12	12.3926	1.27	12.1802	0.04	12.1792	0.04	12.1790	0.04	12.1791	0.04
			TCM/%Err.	25	12.2375	0.00	12.1755	0.00	12.1745	0.00	12.1744	0.00	12.1745	0.00
		Analytical		–	12.2370		12.1752		12.1743		12.1742		12.1742	

Table 8 Fundamental frequency parameters $\bar{\omega} = \omega \frac{a^2}{h}\sqrt{\rho/E_2}$ for SS plate

a/b	a/h	Method		$\bar{N}$	E_1/E_2									
					3		20		30		40		50	
0.5	5	Present	DTM/%Err.	15	4.8399	0.00	8.2401	0.00	8.8813	0.00	9.2832	0.00	9.5660	0.00
			TCM/%Err.	25	4.8399	0.00	8.2401	0.00	8.8813	0.00	9.2832	0.00	9.5660	0.00
		Analytical		–	4.8399		8.2401		8.8813		9.2832		9.5660	
	20	Present	DTM/%Err.	20	5.4774	0.16	12.4005	0.00	14.7975	0.00	16.7100	0.00	18.3070	0.00
			TCM/%Err.	25	5.4685	0.00	12.4009	0.00	14.7974	0.00	16.7105	0.00	18.3073	0.00
		Analytical		–	5.4685		12.4009		14.7974		16.7105		18.3073	
	50	Present	DTM/%Err.	14	5.5000	−0.23	12.9060	0.20	15.6250	0.00	17.9240	0.00	19.9300	−0.02
			TCM/%Err.	25	5.5126	0.00	12.8804	0.00	15.6247	0.00	17.9239	0.00	19.9333	0.00
		Analytical		–	5.5126		12.8804		15.6246		17.9239		19.9333	
1.0	5	Present	DTM/%Err.	17	6.1425	0.00	9.0458	0.00	9.7339	0.00	10.1864	0.00	10.5121	0.00
			TCM/%Err.	25	6.1425	0.00	9.0458	0.00	9.7339	0.00	10.1864	0.00	10.5121	0.00
		Analytical		–	6.1425		9.0458		9.7339		10.1864		10.5121	
	20	Present	DTM/%Err.	19	7.2200	0.01	13.2500	−0.13	15.5840	0.00	17.4835	0.00	19.1000	0.00
			TCM/%Err.	25	7.2194	0.00	13.2676	0.00	15.5846	0.00	17.4839	0.00	19.1002	0.00
		Analytical		–	7.2194		13.2676		15.5845		17.4839		19.1002	
	50	Present	DTM/%Err.	12	7.3000	−0.02	13.7600	0.17	16.3772	0.18	18.6072	0.19	20.5765	0.19
			TCM/%Err.	25	7.3012	0.00	13.7360	0.00	16.3474	0.00	18.5726	0.00	20.5377	0.00
		Analytical		–	7.3012		13.7360		16.3474		18.5726		20.5377	
2.0	5	Present	DTM/%Err.	16	10.9975	0.00	12.3588	0.00	12.9019	0.00	13.3277	0.00	13.6720	0.00
			TCM/%Err.	25	10.9975	0.00	12.3588	0.00	12.9019	0.00	13.3277	0.00	13.6720	0.00
		Analytical		–	10.9975		12.3588		12.9019		13.3277		13.6720	
	20	Present	DTM/%Err.	16	14.9795	0.02	18.4740	0.00	20.2036	0.00	21.7469	0.00	23.1428	0.00
			TCM/%Err.	25	14.9773	0.00	18.4742	0.00	20.2036	0.00	21.7468	0.00	23.1427	0.00
		Analytical		–	14.9772		18.4742		20.2036		21.7468		23.1427	
	50	Present	DTM/%Err.	13	15.3502	−0.19	19.2156	0.09	21.1663	0.11	22.9120	−0.01	24.5480	−0.01
			TCM/%Err.	25	15.3796	0.00	19.1992	0.00	21.1436	0.00	22.9151	0.00	24.5504	0.00
		Analytical		–	15.3796		19.1992		21.1436		22.9151		24.5504	

Table 9 Fundamental frequency parameters $\bar{\omega} = \omega \frac{a^2}{h}\sqrt{\rho/E_2}$ for SC plate

a/b	a/h	Method		$\bar{N}$	E_1/E_2									
					3		20		30		40		50	
0.5	5	Present	DTM/%Err.	29	6.5400	0.74	9.7814	0.11	10.2926	0.02	10.6329	0.01	10.8923	0.00
			TCM/%Err.	25	6.4920	0.00	9.7709	0.00	10.2901	0.00	10.6323	0.00	10.8921	0.00
		Analytical		–	6.4917		9.7709		10.2901		10.6323		10.8921	
	20	Present	DTM/%Err.	21	8.0500	0.11	18.2250	−0.02	21.3750	0.05	23.7500	0.13	25.7900	0.80
			TCM/%Err.	25	8.0418	0.01	18.2310	0.01	21.3647	0.01	23.7211	0.01	25.5865	0.01
		Analytical		–	8.0410		18.2286		21.3634		23.7191		25.5851	
	50	Present	DTM/%Err.	13	8.1750	0.07	19.9270	0.86	23.9440	0.07	27.4445	0.28	30.4350	0.34
			TCM/%Err.	25	8.1692	0.00	19.7581	0.01	23.9296	0.01	27.3706	0.01	30.3356	0.01
		Analytical		–	8.1690		19.7562		23.9265		27.3668		30.3311	
1.0	5	Present	DTM/%Err.	30	7.5297	0.82	10.6965	0.08	11.2745	0.02	11.6554	0.00	11.9400	0.00
			TCM/%Err.	25	7.4689	0.00	10.6878	0.00	11.2725	0.00	11.6549	0.00	11.9399	0.00
		Analytical		–	7.4686		10.6878		11.2725		11.6549		11.9399	
	20	Present	DTM/%Err.	22	9.3740	−0.51	19.1240	0.38	22.3250	0.23	24.8120	0.20	26.9144	0.51
			TCM/%Err.	25	9.4227	0.01	19.0526	0.01	22.2747	0.00	24.7638	0.00	26.7789	0.01
		Analytical		–	9.4219		19.0510		22.2738		24.7632		26.7775	
	50	Present	DTM/%Err.	15	9.4265	−1.70	20.5705	0.74	24.5450	0.07	27.9880	0.10	30.8850	−0.18
			TCM/%Err.	25	9.5900	0.00	20.4210	0.01	24.5305	0.01	27.9616	0.01	30.9441	0.01
		Analytical		–	9.5898		20.4197		24.5288		27.9597		30.9416	
2.0	5	Present	DTM/%Err.	21	11.6520	0.37	13.8598	0.27	14.4964	0.16	14.9477	0.10	15.2933	0.06
			TCM/%Err.	25	11.6092	0.00	13.8229	0.00	14.4727	0.00	14.9333	0.00	15.2847	0.00
		Analytical		–	11.6089		13.8229		14.4727		14.9333		15.2847	
	20	Present	DTM/%Err.	19	16.3940	0.46	23.3000	0.21	26.2455	0.18	28.7151	0.18	30.8502	0.22
			TCM/%Err.	25	16.3198	0.01	23.2521	0.00	26.1978	0.00	28.6630	0.00	30.7814	0.00
		Analytical		–	16.3187		23.2516		26.1972		28.6627		30.7812	
	50	Present	DTM/%Err.	15	16.8825	0.36	24.6202	−0.10	28.2062	0.03	31.3150	0.02	34.1000	−0.01
			TCM/%Err.	25	16.8221	0.00	24.6442	0.00	28.1982	0.00	31.3105	0.00	34.1033	0.00
		Analytical		–	16.8218		24.6437		28.1975		31.3099		34.1026	

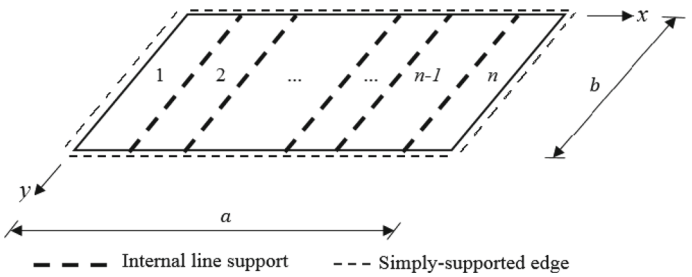

Fig. 2 Multi-span plate (thickness not shown) consisting of $(n-1)$ internal supports

Table 10 Frequency $\bar{\omega} = \omega \frac{a^2}{h}\sqrt{\rho/E_2}$ for a three-span plate with $\frac{a}{b} = 3.0$, $\frac{a}{h} = 10$ and $\frac{E_1}{E_2} = 5$

Method	CPT		FSDT		HSDT		RPT	
	$\bar{N}$	$\bar{\omega}$	$\bar{N}$	$\bar{\omega}$	$\bar{N}$	$\bar{\omega}$	$\bar{N}$	$\bar{\omega}$
DTM	7	8.6465	9	7.5464	6	7.6435	7	9.5287
	9	8.1837	11	7.6452	8	7.7756	9	7.7513
	11	8.2887	13	7.8102	10	7.8248	11	7.8415
	12	8.2887	14	7.8202	11	7.8284	12	7.8415
TCM	6	8.3017	5	7.8096	5	7.8240	6	7.8521
	8	8.2783	7	7.8316	7	7.8343	8	7.8322
	10	8.2788	9	7.8309	9	7.8342	10	7.8327
	11	8.2788	10	7.8309	10	7.8342	11	7.8327

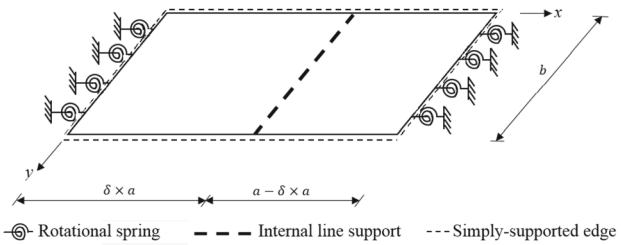

Fig. 3 A two-span plate (thickness not shown) with end rotational springs of stiffness $\bar{k}_s$

Table 11 Frequency $\bar{\omega} = \omega \frac{a^2}{h}\sqrt{\rho/E_2}$ for a two-span plate and plate with stepped thickness and end rotational springs: $\frac{a}{b} = 3.0$, $\frac{a}{h} = 10$ and $\frac{E_1}{E_2} = 5$

Plate type	$\bar{k}_s$	Method	CPT		FSDT		HSDT		RPT	
			$\bar{N}$	$\bar{\omega}$	$\bar{N}$	$\bar{\omega}$	$\bar{N}$	$\bar{\omega}$	$\bar{N}$	$\bar{\omega}$
Two span (Fig. 3)	0	DTM	11	11.2056	12	10.4024	14	10.4047	13	10.4034
		TCM	10	11.1869	10	10.4050	9	10.4042	10	10.4035
	5	DTM	11	13.4678	12	12.4133	11	12.4218	12	12.4533
		TCM	12	13.7681	9	12.4211	11	12.4200	10	12.4221
Plate with two thickness steps	0	DTM	19	9.9732	23	8.8001	21	8.7432	23	8.8001
		TCM	20	10.0185	23	8.7446	23	8.7511	23	8.7831
	5	DTM	21	16.5312	23	15.2061	25	15.2210	23	15.2356
		TCM	22	16.2456	24	15.2112	23	15.2300	24	15.2420

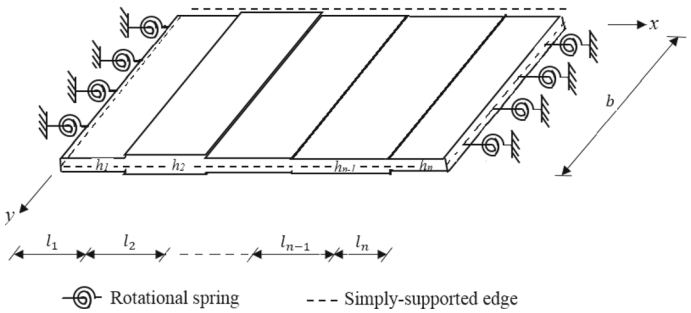

Fig. 4 Plate with stepped thickness ("n" segments) and end rotational springs of stiffness $\bar{k}_s$

the moment boundary conditions at the two edges (i.e., at $x = 0$ and $x = a$) in the case of plates with rotational springs needs to be modified. These modifications are given by Eqs. (67) and (68) and are applied to both the two-span plate with end springs and the plate with stepped thickness and end springs above.

It is clear in all the three problems presented in this section that the RPT-based DTM and TCM predicts the frequency factors that agree closely with the HSDT with marginal differences on the conservative side, whereas the CPT overestimates these factors. It is interesting to note that since TCM is fully numerical, it turns out to be more flexible than DTM which is semi-analytical in nature. As a result, the former can be applied (but with different formulation from the one presented in this work) to handle non-classic (non-canonic) plate shapes, while the applicability of the latter for such cases needs to be established by further research.

$$(w_b)_i = (w_b)_{i+1} \tag{59}$$

$$(w_s)_i = (w_s)_{i+1} \tag{60}$$

$$\left(w_b'\right)_i = \left(w_b'\right)_{i+1} \tag{61}$$

$$\left(w_s'\right)_i = \left(w_s'\right)_{i+1} \tag{62}$$

$$\left(-D_{11}w_b'' + D_{12}\beta^2 w_b\right)_i = \left(-D_{11}w_b'' + D_{12}\beta^2 w_b\right)_{i+1} \tag{63}$$

$$\left(-(1/84)\left(D_{11}w_s'' - D_{12}\beta^2 w_s\right)\right)_i = \left(-(1/84)\left(D_{11}w_s'' - D_{12}\beta^2 w_s\right)\right)_{i+1} \tag{64}$$

$$\left(-D_{11}w_b''' + \left(\left(D_{12}+4D_{66}\right)\beta^2 - I_2\omega_n^2\right)w_b'\right)_i = \left(-D_{11}w_b''' + \left(\left(D_{12}+4D_{66}\right)\beta^2 - I_2\omega_n^2\right)w_b'\right)_{i+1} \tag{65}$$

$$\left(-D_{11}w_s''' + \left(\left(D_{12}+4D_{66}\right)\beta^2 - I_2\omega_n^2 + 84A_{55}\right)w_s'\right)_i = \left(-D_{11}w_s''' + \left(\left(D_{12}+4D_{66}\right)\beta^2 - I_2\omega_n^2 + 84A_{55}\right)w_s'\right)_{i+1} \tag{66}$$

$$-D_{11}w_b'' + D_{12}\beta^2 w_b = \bar{k}_s w_b' \tag{67}$$

$$-(1/84)\left(D_{11}w_s'' - D_{12}\beta^2 w_s\right) = \bar{k}_s w_s' \tag{68}$$

6 Conclusions

In this paper, free vibration analysis of orthotropic plates has been carried out using the differential transform method (DTM) and Taylor collocation method (TCM) based on the two-variable refined plate theory. Detailed formulations of the methods have been given, followed by their implementation on plates having different end conditions. The results have been verified using the analytical solution in cases of SS, SC and SF plates based on the same theory, and consequently, various factors ranging from geometric to material parameters have been studied. Cases of multi-span plates and plates with stepped thickness and end rotational springs were also studied in order to show the capability of the proposed methods and the plate theory, the RPT, in solving problems whose analytical solutions are not readily available. Comparison have also been made with the results based on other plate theories, such as the classical plate theory, the first-order shear deformation theory and the high-order shear deformation theory. In light of the outcome of the analyses, the following conclusions can be drawn.

1. Although the classical plate theory is the simplest and most appealing compared to other shear deformation theories, and since it cannot be relied upon in all situations, the two-variable refined plate theory serves as a good alternative since its formulation is relatively simple and resembles that of the classical plate theory, and yet it takes into account the effect of shear deformation. In addition, the resulting system of equations are easier to solve than those of other higher order theories.
2. Contrary to the case of some shear deformation theories, the present theory does not require any shear correction factor and it results in quadratic distribution of the shear stress satisfying zero-traction boundary condition at the top and bottom surfaces of the plate.
3. Compared to the present theory, the classical plate theory overestimates the natural frequencies.
4. Capability of DTM and TCM to analyze orthotropic plates has been proven, and good agreement exists between the results achieved and the analytical ones for SS, SC and SF plates on the one hand, and the FSDT and HSDT for multi-span plates and plates with stepped thickness and end rotational springs on the other.
5. In cases of SS, SC and SF plates based on CPT, accuracy level of both DTM and TCM is the same. However, based on RPT, results obtained from TCM are, in few cases, better (though not significantly different from the DTM). On the other hand, the DTM requires less computer memory in its solution because the final size of the system matrix is much smaller than that needed to be handled in the TCM. For example, while solution for SF, SS and SC plates using the DTM requires dealing with just a 4×4 matrix, the TCM requires one to deal with a $2\left(\bar{N}+1\right) \times 2\left(\bar{N}+1\right)$ matrix for the same plates.
6. The effect of increasing the aspect ratio and thickness ratio is to cause a corresponding increase in the fundamental natural frequency parameter, hence, increase in the fundamental natural frequency for all the plate types studied.
7. The effect of increasing the modular ratio causes an increase in the fundamental natural frequency parameter for the SS and SC plates. On the other hand, no such effect is observed in the case of SF plate because of its free end which lowers the plate's stiffness.
8. Denoting the fundamental natural frequency parameters for the SF, SS and SC plates as $\bar{\omega}_{SF}$, $\bar{\omega}_{SS}$ and $\bar{\omega}_{SC}$, it can be seen that under the same condition (same thickness ratio, aspect ratio and modular ratio), values of the fundamental natural frequency parameters have magnitudes in the order $\bar{\omega}_{SC} > \bar{\omega}_{SS} > \bar{\omega}_{SF}$. Similar finding is confirmed in [73].
9. Both the two numerical methods, DTM and TCM, adopted in obtaining these solutions do not require iterations as is the case with the analytical results reported in [35].
10. Unlike other element-based numerical techniques, the DTM and TCM can be used to present solutions in symbolic forms which warrants the possibility of obtaining other secondary variables by differentiation, integration, etc.

11. The obvious advantage of eliminating the need for method calibration as required in other meshless methods, such as the Kansa method and method of fundamental solutions, adds to the appealing nature of the presented methods.

Acknowledgements The author would like to acknowledge the support of King Fahd University of Petroleum & Minerals (KFUPM).

Appendix

Coefficients a_{ij}, $\{i, j = 1, 2, 3, 4\}$ appearing in the DTM-based system matrix given in Eq. (33).

SC—Plate:

$$a_{11} = \left(\frac{1}{\sum_{k=3}^{N} \text{Coeff.}\left[W_b\left(k\right), \zeta_b\right]} + 1\right), \qquad a_{1j} = 1, \qquad j = 2, 3, 4$$

$$a_{22} = \left(\frac{1}{\sum_{k=3}^{N} \text{Coeff.}\left[W_s\left(k\right), \eta_b\right]} + 1\right), \qquad a_{2j} = 1, \qquad j = 1, 3, 4$$

$$a_{33} = \left(\frac{1}{\sum_{k=3}^{N} \text{Coeff.}\left[W_b\left(k\right), \zeta_s\right]} + 1\right), \qquad a_{3j} = \sum_{k=1}^{N} k, \qquad j = 1, 2, 4$$

$$a_{44} = \left(\frac{1}{\sum_{k=3}^{N} \text{Coeff.}\left[W_s\left(k\right), \eta_s\right]} + 1\right), \qquad a_{4j} = \sum_{k=1}^{N} k, \qquad j = 1, 2, 3$$

SS—Plate:

$$a_{1j} = 1, \qquad j = 1, 2, 3, 4$$

$$a_{2j} = 1, \qquad j = 1, 2, 3, 4$$

$$a_{31} = \frac{D_{12}\beta^2}{\sum_{k=2}^{N} \text{Coeff.}\left[W_b\left(k\right), \zeta_b\right]} + \left(-D_{11}\sum_{k=2}^{N} k\left(k-1\right) + D_{12}\beta^2\right)$$

$$a_{3j} = -D_{11}\sum_{k=2}^{N} k\left(k-1\right) + D_{12}\beta^2, \quad j = 2, 3, 4$$

$$a_{41} = -\left(\frac{1}{84}\right)\left[\frac{-D_{12}\beta^2}{\sum_{k=2}^{N} \text{Coeff.}\left[W_s\left(k\right), \zeta_b\right]} + \left(D_{11}\sum_{k=2}^{N} k\left(k-1\right) - D_{12}\beta^2\right)\right]$$

$$a_{4j} = -\left(\frac{1}{84}\right)\left(D_{11}\sum_{k=2}^{N} k\left(k-1\right) - D_{12}\beta^2\right), \quad j = 2, 3, 4$$

SF—Plate:

$$a_{11} = \left(\frac{D_{12}\beta^2}{\sum_{k=3}^{N} W_b\left(k\right)} + D_{12}\beta^2 - D_{11}\sum_{k=3}^{N} k\left(k-1\right)\right),$$

$$a_{1j} = D_{12}\beta^2 - D_{11}\sum_{k=3}^{N} k\left(k-1\right), \quad j = 2, 3, 4$$

$$a_{23} = -\left(\frac{1}{84}\right)\left(-\frac{D_{12}\beta^2}{\sum_{k=3}^{N} W_s\left(k\right)} - D_{12}\beta^2 + D_{11}\sum_{k=3}^{N} k\left(k-1\right)\right),$$

$$a_{2j} = -\left(\frac{1}{84}\right)\left(-D_{12}\beta^2 + D_{11}\sum_{k=3}^{N} k\,(k-1)\right), \quad j = 1, 2, 4$$

$$a_{31} = \left[\left(\left(D_{12} + 4D_{66}\right)\beta^2 - I_2\omega_n^2\right)\left(\frac{1}{\sum_{k=3}^{N} W_b\,(k)} + \sum_{k=3}^{N} k\right) - D_{11}\sum_{k=3}^{N} k\,(k-1)\,(k-2)\right]$$

$$a_{3j} = \left[\left(\left(D_{12} + 4D_{66}\right)\beta^2 - I_2\omega_n^2\right)\left(\sum_{k=3}^{N} k\right) - D_{11}\sum_{k=3}^{N} k\,(k-1)\,(k-2)\right], \quad j = 2, 3, 4$$

$$a_{41} = \left[\left(\left(D_{12} + 4D_{66}\right)\beta^2 - I_2\omega_n^2 + 84A_{55}\right)\left(\frac{1}{\sum_{k=3}^{N} W_b\,(k)} + \sum_{k=3}^{N} k\right) - D_{11}\sum_{k=3}^{N} k\,(k-1)\,(k-2)\right]$$

$$a_{4j} = \left[\left(\left(D_{12} + 4D_{66}\right)\beta^2 - I_2\omega_n^2 + 84A_{55}\right)\left(\sum_{k=3}^{N} k\right) - D_{11}\sum_{k=3}^{N} k\,(k-1)\,(k-2)\right], \quad j = 2, 3, 4$$

References

1. Kirchhoff, G.R.: Uber das gleichgewicht und die bewegung einer elastischen Scheibe. J. Reine Angew Math. (Crelle's J) **40**, 51–88 (1850)
2. Tret'yak, V.G.: Natural vibrations of orthotropic plates. Sov. Appl. Mech. **2**, 27–31 (1966)
3. Sakata, T., Hosokawa, K.: Vibrations of clamped orthotropic rectangular plates. J. Sound Vib. **125**, 429–439 (1988)
4. Jayaraman, G., Chen, P., Snyder, V.W.: Free vibrations of rectangular orthotropic plates with a pair of parallel edges simply supported. Comput. Struct. **34**, 203–214 (1990)
5. Harik, I.E., Liu, X., Balakrishnan, N.: Analytic solution to free vibration of rectangular plates. J. Sound Vib. **153**, 51–62 (1992)
6. Biancolini, M.E., Brutti, C., Reccia, L.: Approximate solution for free vibrations of thin orthotropic rectangular plates. J. Sound Vib. **288**, 321–344 (2005)
7. Xing, Y.F., Liu, B.: New exact solutions for free vibrations of thin orthotropic rectangular plates. Compos. Struct. **89**, 567–574 (2009)
8. Reissner, E.: On the theory of bending of elastic plates. J. Math. Phys. **23**, 184–191 (1944)
9. Reissner, E.: The effect of transverse shear deformation on the bending of elastic plates. ASME J. Appl. Mech. **12**, A69–A77 (1945)
10. Mindlin, R.D.: Influence of rotatory inertia and shear on flexural motions of isotropic, elastic plates. ASME J. Appl. Mech. **18**, 31–38 (1951)
11. Nelson, R.B., Lorch, D.R.: A refined theory for laminated orthotropic plates. ASME J. Appl. Mech. **41**, 177–183 (1974)
12. Murty, A.V.K.: Higher order theory for vibrations of thick plates. AIAA J. **15**, 1823–1824 (1977)
13. Lo, K.H., Christensen, R.M., Wu, E.M.: A high-order theory of plate deformation. Part 1: homogeneous plates. ASME J. Appl. Mech. **44**, 663–668 (1977)
14. Lo, K.H., Christensen, R.M., Wu, E.M.: A high-order theory of plate deformation. Part 2: laminated plates. ASME J. Appl. Mech. **44**, 669–676 (1977)
15. Kant, T.: Numerical analysis of thick plates. Comput. Meth. Appl. M. **31**, 1–18 (1982)
16. Bhimaraddi, A., Stevens, L.K.: A higher order theory for free vibration of orthotropic, homogeneous, and laminated rectangular plates. ASME J. Appl. Mech. **51**, 195–198 (1984)
17. Reddy, J.N.: A refined nonlinear theory of plates with transverse shear deformation. Int. J. Solids Struct. **20**, 881–896 (1984)
18. Soldatos, K.P.: On certain refined theories for plate bending. ASME J. Appl. Mech. **55**, 994–995 (1988)
19. Reddy, J.N.: A general non-linear third-order theory of plates with moderate thickness. Int. J. Nonlinear Mech. **25**, 677–686 (1990)
20. Hanna, N.F., Leissa, A.W.: A higher order shear deformation theory for the vibration of thick plates. J. Sound Vib. **170**, 545–555 (1994)
21. Chen, W.C., Liu, W.H.: Deflections and free vibrations of laminated plates-Levy-type solutions. Int. J. Mech. Sci. **32**, 779–793 (1990)
22. Hashemi, S.H., Arsanjani, M.: Exact characteristic equations for some of classical boundary conditions of vibrating moderately thick rectangular plates. Int. J. Solids Struct. **42**, 819–853 (2005)
23. Kshirsagar, S., Bhaskar, K.: Free vibration and stability analysis of orthotropic shear-deformable plates using untruncated infinite series superposition method. Thin Wall. Struct. **47**, 403–411 (2009)
24. Lim, C.W., Lü, C.F., Xiang, Y., Yao, W.: On new symplectic elasticity approach for exact free vibration solutions of rectangular Kirchhoff plates. Int. J. Eng. Sci. **47**, 131–140 (2009)
25. Oktem, A.S., Chaudhuri, R.A.: Levy type analysis of cross-ply plates based on higher-order theory. Compos. Struct. **78**, 243–253 (2007)
26. Kant, T., Swaminathan, K.: Free vibration of isotropic, orthotropic, and multilayer plates based on higher order refined theories. J. Sound Vib. **241**, 319–327 (2001)
27. Hadian, J., Nayfeh, A.H.: Free vibration and buckling of shear-deformable cross-ply laminated plates using the state-space concept. Comput. Struct. **48**, 677–693 (1993)

28. Reddy, J.N., Phan, N.D.: Stability and vibration of isotropic, orthotropic and laminated plates according to a higher-order shear deformation theory. J. Sound Vib. **98**, 157–170 (1985)
29. Shimpi, R.P.: Refined plate theory and its variants. AIAA J. **40**, 137–146 (2002)
30. Shimpi, R.P., Patel, H.G.: A two variable refined plate theory for orthotropic plate analysis. Int. J. Solids Struct. **43**, 6783–6799 (2006)
31. Carrera, E.: Historical review of zig-zag theories for multilayered plates and shells. Appl. Mech. Rev. **56**(3), 287–308 (2003)
32. Altenbach, H., Eremeyev, V.: Eigen-vibrations of plates made of functionally graded material. Comput. Mater. Con. **9**(2), 153–178 (2009)
33. Ghugal, Y.M., Pawar, M.D.: Buckling and vibration of plates by hyperbolic shear deformation theory. J. Aerosp. Eng. Technol. **1**, 1–12 (2011)
34. Shimpi, R.P., Patel, H.G.: Free vibrations of plate using two variable refined plate theory. J. Sound Vib. **296**, 979–999 (2006)
35. Thai, H.T., Kim, S.E.: Levy-type solution for free vibration analysis of orthotropic plates based on two variable refined plate theory. Appl. Math. Model. **36**, 3870–3882 (2012)
36. Hull, P.V., Buchanan, G.R.: Vibration of moderately thick square orthotropic stepped thickness plates. Appl. Acoust. **64**, 753–763 (2003)
37. Brischetto, S., Carrera, E.: Importance of higher order modes and refined theories in free vibration analysis of composite plates. ASME J. Appl. Mech. **77**, 011013–011013–14 (2009). doi:10.1115/1.3173605
38. Cetkovic, M., Vuksanovic, D.: Vibrations of isotropic, orthotropic and laminated composite plates with various boundary conditions. J. Serb Soc. Comput. Mech. **6**, 83–96 (2012)
39. Gupta, U.S., Ansari, A.H., Sharma, S.: Buckling and vibration of polar orthotropic circular plate resting on Winkler foundation. J. Sound Vib. **297**, 457–476 (2006)
40. Kumar, Y., Lal, R.: Vibrations of nonhomogeneous orthotropic rectangular plates with bilinear thickness variation resting on Winkler foundation. Meccanica **47**, 893–915 (2012)
41. Lal, R., Kumar, Y.: Characteristic orthogonal polynomials in the study of transverse vibrations of nonhomogeneous rectangular orthotropic plates of bilinearly varying thickness. Meccanica **47**, 175–193 (2012)
42. Ding, H.J., Chen, W.Q., Xu, R.Q.: On the bending, vibration and stability of laminated rectangular plates with transversely isotropic layers. Appl. Math. Mech. **22**, 17–24 (2001)
43. Makhecha, D.P., Ganapathi, M., Patel, B.P.: Vibration and damping analysis of laminated/sandwich composite plates using higher-order theory. J. Reinf. Plast. Comp. **6**, 559–575 (2002)
44. Chen, W.Q., Lu, C.F.: 3D Free vibration analysis of cross-ply laminated plates with one pair of opposite edges simply supported. Compos. Struct. **69**, 77–87 (2005)
45. Sharma, S., Gupta, U.S., Singhal, P.: Vibration analysis of non-homogeneous orthotropic rectangular plates of variable thickness resting on Winkler foundation. J. Appl. Sci. Eng. **15**, 291–300 (2012)
46. Roque, C.M.C., Ferreira, A.J.M., Jorge, R.M.N.: Free vibration analysis of composite and sandwich plates by a trigonometric layerwise deformation theory and radial basis functions. J. Sandw. Struct. Mater. **8**, 497–515 (2006)
47. Wu, C.P., Chiu, K.H.: RMVT-based mesh-less collocation and element free Galerkin methods for the quasi 3D free vibration analysis of multilayered composite and FGM plates. Compos. Struct. **93**, 1433–1448 (2011)
48. Xiang, S., Kang, G.W., Yang, M.S., Zhao, Y.: Natural frequencies of sandwich plate with functionally graded face and homogeneous core. Compos. Struct. **96**, 226–231 (2013)
49. Zhang, Q.J., Sainsbury, M.G.: The Galerkin element method applied to the vibration of rectangular damped sandwich plates. Comput. Struct. **74**, 717–730 (2000)
50. Gorman, D.J.: Free vibration analysis of completely free rectangular plates by the superposition-Galerkin Method. J. Sound Vib. **237**, 901–914 (2000)
51. Wei, G.W., Zhao, Y.B., Xiang, Y.: A novel approach for the analysis of high frequency vibrations. J. Sound Vib. **2**, 207–246 (2002)
52. Zhao, Y.B., Wei, G.W., Xiang, Y.: Discrete Singular convolution for the prediction of high frequency vibration of plates. Int. J. Solids Struct. **39**, 65–88 (2002)
53. Ranji, A.R., Hoseynabadi, H.R.: A semi-analytical solution for forced vibrations response of rectangular orthotropic plates with various boundary conditions. J. Mech. Sci. Technol. **24**, 357–364 (2010)
54. Carrera, E., Brischetto, S.: Analysis of thickness locking in classical, refined and mixed multilayered plate theories. Compos. Struct. **82**, 549–562 (2008)
55. Liu, B., Xing, Y.: Exact solutions for free in-plane vibrations of rectangular plates. Acta Mech. Solida Sin. **24**, 556–567 (2011)
56. Liu, B., Xing, Y.: Exact solutions for free vibrations of orthotropic rectangular Mindlin plates. Compos. Struct. **93**, 1664–1672 (2011)
57. Sayyad, A.S., Ghugal, Y.M.: On the free vibration analysis of laminated composite and sandwich plates: a review of recent literature with some numerical results. Compos. Struct. **129**, 177–201 (2015)
58. Yalcin, H.S., Arikoglu, A., Ozkol, I.: Free vibration analysis of circular plates by differential transformation method. Appl. Math. Comput. **212**, 377–386 (2009)
59. Semnani, S.J., Attarnejad, R., Firouzjaei, R.K.: Free vibration analysis of variable thickness thin plates by two-dimensional differential transform method. Acta Mech. **224**, 1643–1658 (2013)
60. Mindlin, R.D., Schacknow, A., Deresiewicz, H.: Flexural vibration of rectangular plates. J. Appl. Mech. **23**, 430–436 (1956)
61. Chen, W.C., Liu, W.H.: Deflections and free vibrations of laminated plates–Levy-type solutions. Int. J. Mech. Sci. **32**, 779–793 (1990)
62. Sayyad, A.S., Ghugal, Y.M.: Buckling and free vibration analysis of orthotropic plates by using exponential shear deformation theory. Latin Am. J. Solids Struct. **11**, 1298–1314 (2014)
63. Kienzler, R.: On consistent plate theories. Arch. Appl. Mech. **72**, 229–247 (2002)
64. Schneider, P., Kienzler, R., Böhm, M.: Modeling of consistent second-order plate theories for anisotropic materials. Z. Angew. Math. Mech. **94**(1–2), 21–42 (2014)

65. Schneider, P., Kienzler, R.: Comparison of various linear plate theories in the light of a consistent second-order approximation. Math. Mech. Solids **20**(7), 871–882 (2015)
66. Zhou, J.K.: Differential Transformation and its Applications for Electrical Circuits. Huazhong University Press, Wuhan (1986)
67. Chen, F.C., Young, K.: Inclusions of arbitrary shape in an elastic medium. J. Math. Phys. **18**, 1412–1416 (1977)
68. Kanwal, R.P., Liu, K.C.: A Taylor expansion approach for solving integral equations. Int. J. Sci. Math. Educ. **20**, 411–414 (1989)
69. Sezer, M.: Taylor polynomial solutions of volterra integral equations. Int. J. Math. Educ. Sci. Technol. **25**, 625–633 (1994)
70. Mukhtar, F.M.: Generalized Taylor polynomials for axisymmetric plates and shells. Appl. Math. Comput. **276**, 182–199 (2016)
71. Srinivas, S., Rao, A.: Bending, vibration and buckling of simply supported thick orthotropic rectangular plates and laminates. Int. J. Solids Struct. **6**, 1463–1481 (1970)
72. Reddy, J.N.: Mechanics of Laminated Composite Plates and Shells: Theory and Analysis. CRC Press, Boca Raton (2004)
73. Eremeyev, V.A., Lebedev, L.P., Cloud, M.J.: The Rayleigh and Courant variational principles in the six-parameter shell theory. Math. Mech. Solids **20**(7), 806–822 (2015)